Insight into the Hydrogen Migration Processes Involved in the Formation of Metal-Borane Complexes: The Importance of the Third Arm of the Scorpionate Ligand

*Nikolaos Tsoureas, Alex Hamilton, Mairi F. Haddow, Jeremy N. Harvey, A. Guy Orpen and Gareth R. Owen,**†

The School of Chemistry, University of Bristol, Cantock's Close, Bristol, UK, BS8 1TS

Gareth.Owen@bristol.ac.uk

RECEIVED DATE

Dr. Gareth R. Owen, Royal Society Dorothy Hodgkin Research Fellow, University of Bristol. Tel: 44 (0)117 928 8162; E-mail: gareth.owen@bristol.ac.uk

† Royal Society Dorothy Hodgkin Research Fellow

ABSTRACT

The reactions of [Ir(κ^3-*NNH*-**Tai**)(COD)] and [Ir(κ^3-*NNH*-^{Ph}**Bai**)(COD)] {where **Tai** = HB(azaindolyl)$_3$ and ^{Ph}**Bai** = Ph(H)B(azaindolyl)$_2$} with carbon monoxide result in the formation of *Z*-type iridium-borane complexes supported by 7-azaindole units. Analysis of the reaction mixtures involving the former complex revealed the formation of a single species in solution, [Ir(η^1-C_8H_{13}){κ^3-*NNB*-B(azaindolyl)$_3$}$(CO)_2$], as confirmed by NMR spectroscopy. In the case of the ^{Ph}**Bai** complex, a mixture of species was observed. A postulated mechanism for the formation of the new complexes has been provided supported by computational studies. Computational studies have also focused on the reaction

step involving the migration of hydrogen from boron (in the borohydride group) to the iridium center. These investigations have demonstrated a small energy barrier for the hydrogen migration step (ΔG_{298} = 10.3 kcal mol^{-1}). Additionally, deuterium labeling of the borohydride units in **Tai** and ^{Ph}**Bai** confirmed the final position of the former borohydride hydrogen atom in the resulting complexes. The importance of the 'third azaindolyl' unit within these transformations and the difference in reactivity between the two ligands are discussed. The selective coordination properties this family of metallaboratrane complexes has also been investigated and is discussed herein.

MANUSCRIPT TEXT

Introduction

Flexible new generation scorpionate ligands, i.e. borate ligands which possess two atoms between the boron and donor atom, have received considerable interest over the past decade or so due in part to their extraordinary reactivity at the boron center.[1] The first such ligand, **Tm** [hydrotris(2-mercapto-1-methyl-imidazolyl)borate], was introduced by Reglinski in 1996.[2] The implications of the increased flexibility of the ligands were realized by the isolation of Hill's inaugural metallaboratrane complex;[1] the first complex to spark interest and popularize the field of Z-type coordination.[3] Since their discovery in 1999, metal-borane complexes have attracted considerable attention captivating the imagination of researchers in the fields of coordination and organometallic chemistry.[4,5] There are no authenticated examples of κ^1*B* (Z-type) complexes,[6] and it is currently believed that at least one supporting group is required to tether the borane functionality to the metal center.[7] Chart 1 highlights some of the three atom bridging units which have been employed to support metal-borane complexes. While the majority of examples are based on soft donors atom scaffolds (sulfur[8] and phosphines[7,9]), we have reported examples based on nitrogen utilizing the heterocycle 7-azaindole.[10] Further development and rapid expansion of the field of Z-type complexes has resulted in many new and novel interactions where a transition metal center acts as a Lewis base.[11,12]

Chart 1 – Common three atom bridging units which have been employed to support metal-borane complexes [all other substituents at boron (B) and metal centre (M) have been omitted for clarity].

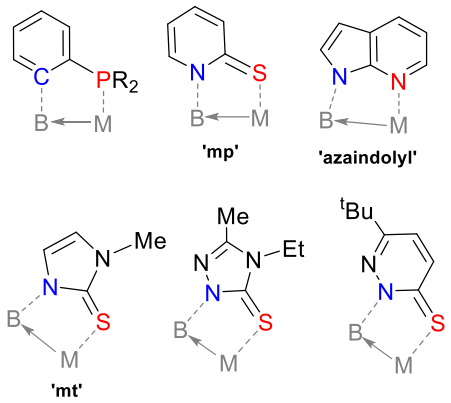

Our recent investigations have been primarily focused on the utilization of metal-borane complexes as potential '*hydrogen atom stores*'[4a] (Scheme 1). Accordingly, we have reported a number of cases involving hydrogen atom migration from a borohydride unit, eventually leading to its incorporation into an organic moiety already coordinated to the metal center (**1** – **3** in Chart 2).[8c,10b,c] We have also reported a system where the hydrogen atom was '*locked*' at an intermediate point between boron and metal centers (ruthenium complex **3**).[13] One of the ligands we have concentrated on in our investigations is scorpionate ligand **Tai** [hydrotris(7-azaindolyl)borate],[14] a flexible analogue of Trofimenko's ubiquitous polypyrazolylborate ligands.[15] For example, the complex [Rh{κ^3-*NNH*-HB(azaindolyl}$_3$(NBD)] (NBD = 2,5-norbornadiene) converts to the metallaboratrane complex [Rh(nortricyclyl){κ^4-*NNBN*-B(azaindolyl)$_3$}] (**1** in Chart 2) via an initial hydrogen migration step and subsequent double bond migration.[10c] In this case, it appears that the strain associated with the diene moiety norbornadiene is the driving force for migration. Interestingly, it was later shown that the boron center in **1** could be '*recharged*' back to the borohydride functionality upon reaction with H_2 providing an active hydrogenation catalyst.[10a,16]

Scheme 1 – Reversible hydrogen atom migration between boron and metal centers

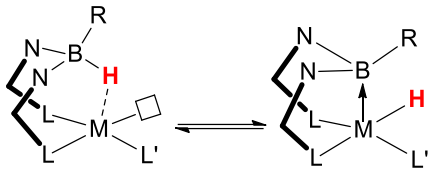

Chart 2 – Incorporation of the borohydride hydrogen atom into various organic fragments; the colored hydrogen atoms highlight the endpoint of the former borohydride hydrogen atoms (N—N = azaindolyl, N—S' = mp and N—S = mt).

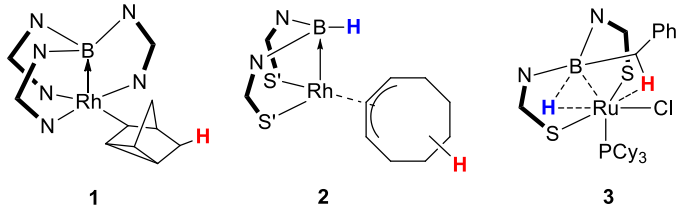

1 **2** **3**

In an effort to further explore the concept of the boron based hydrogen mobility, we began to investigate new derivatives of **Tai** where one of the three azaindolyl units was replaced by a non-coordinating group. Accordingly, the ligands $[(Ar)HB(azaindolyl)_2]^-$ (**^{Ar}Bai**; where Ar = phenyl, mesityl and naphthyl) were synthesized along with some preliminary complexes.[10c,17,18] During our investigations, we established a new methodology to trigger hydrogen migration by disturbing the coordination sphere of the complex. A preliminary account of this work, including the complete characterization of two complexes (**6** and **11**), has previously been communicated[10b] and we therefore wish to report further results and details from our investigations. Herein, we report i) further details and new examples adding to the family of metal-borane complexes supported by nitrogen based supporting groups, ii) experimental and computational evidence supporting a carbon monoxide assisted mechanism, iii) further insight into the hydrogen migration process between boron and metal center and iv) our investigations probing the coordination properties of the site trans to boron center.

Results

Reactions involving hydrotris(azaindolyl)borate, Tai An investigation was initiated involving ligand substitution reactions on the previously reported complex, [Ir{κ^3-*NNH*-HB(azaindolyl)}$_3$(COD)] (**4**) (Scheme 2).[14c] Literature precedent had suggested that the cyclooctadiene unit could readily be substituted by two carbonyl ligands to form the expected complex [Ir{κ^3-*NNH*-HB(azaindolyl)}$_3$(CO)$_2$].[19] Accordingly, complex **4** was dissolved in toluene-d$_8$ in a Young's NMR tube and placed under a slight overpressure of CO (*ca*. 1.5 bar). The color of the solution changed from yellow to colorless over a period of 5 minutes. The ^{11}B{^{1}H} NMR spectrum of the mixture confirmed the full conversion to an unexpected product **5**, where the former borohydride hydrogen atom has been incorporated into the eight membered organic group (Scheme 2).

Scheme. 2 – Synthesis of complexes **5** upon reaction of **4** with $CO_{(g)}$. Complex **5** looses one equivalent of CO upon workup (reduced pressure) to form **6**.

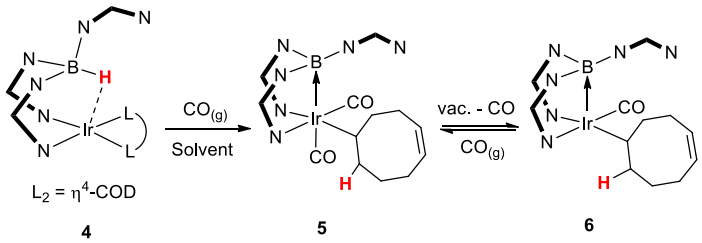

The new complex **5**, was confirmed as [Ir(η^1-C$_8$H$_{13}$){κ^3-*NNB*-B(azaindolyl)$_3$}(CO)$_2$] on the basis of the spectroscopic data. Some aspects of the spectroscopic data for **5** have previously been described.[10b] The ^{1}H NMR spectrum revealed the clean formation of a new product, with the aromatic region integrating for 15 protons indicating three inequivalent environments for the azaindole rings. The spectrum further showed two overlapping multiplet signals centered at 5.46 ppm (integrating for 2 protons collectively) corresponding to uncoordinated protons of the alkene functional group. A number of broad multiplet signals were also found in the region of the spectrum between 2.3 and 1.0 ppm integrating for 10 protons. A further broad signal was additionally located at –0.07 ppm and was identified as one of the CH_2 protons in the β-position of the Ir–cyclooctenyl group (*via* an HMQC-NMR experiment). The high field chemical shift of this signal suggests a close interaction of this proton with the iridium center. The product was further characterized by ^{13}C{^{1}H} NMR spectroscopy. The spectrum

revealed the expected 21 sharp signals for the three azaindole units and 2 olefinic carbons between 101.3 and 156.8 ppm. Additionally, six resonances in the aliphatic region between 46.2 and 17.0 ppm were observed in the spectrum as expected (vide infra). The most upfield chemical shift was assigned as the carbon atom bound to the iridium center as confirmed by a DEPT-135 NMR experiment. An HMQC correlation experiment revealed that the Ir–C*H* proton signal was located at 1.7 ppm and overlapped with some of the other alkylic signals. The presence of two signals at 179.1 and 170.0 ppm in the $^{13}C\{^{1}H\}$-NMR spectrum confirmed the coordination of two inequivalent carbonyl ligands at the iridium center. The infrared spectrum of the reaction mixture also confirmed the coordination of CO ligands to the metal center.

As we previously reported, our attempts to isolate **5** on a preparative scale were unsuccessful and a different product was obtained after standard reaction work-up (Scheme 2). An air-stable pale yellow solid **6**, was isolated from the reaction mixture and was fully characterized by NMR and IR spectroscopies, ESI mass spectrometry and elemental analysis. The ^{1}H NMR spectrum (in toluene-d_8) also revealed the clean formation of a new product, with three environments for the azaindole rings. The spectrum further indicated two signals centered at 5.45 and 5.61 ppm (each integrating for 1 proton) corresponding to uncoordinated alkene protons. As with the case of **5**, no further signals corresponding to either coordinated or uncoordinated alkene were observed in the spectrum. The aliphatic region of the spectrum again showed a number of broad signals with a total integration of 11 protons. Interestingly, the signal observed at −0.07 ppm for complex **5** appeared shifted downfield to 0.85 ppm in the case of complex **6**. Again, the product was further characterized by $^{13}C\{^{1}H\}$ NMR spectroscopy.[20] In contrast to the spectrum of **5**, only one signal corresponding to CO was observed at 173.1 ppm. The coordination of this CO ligand was further confirmed by IR spectroscopy which revealed a strong intensity band at 1984 cm^{-1} in the solid state and a medium intensity band at 2008 cm^{-1} in toluene solution (or 2011 cm^{-1} in THF). The molecular composition of **6** was confirmed by elemental analysis and mass spectrometry. The latter gave peaks at 585.1 a.m.u. $[M - C_8H_{13}]^+$, 693.2 a.m.u. $[M + H]^+$, 715.2 a.m.u. $[M + Na]^+$ which were in agreement with the theoretically calculated isotopic pattern distributions. Single crystals of **6** were obtained and the molecular structure confirmed our assignment of **6** as [Ir(η^1-C_8H_{13}){κ^3-*NNB*-

B(azaindolyl)$_3$}(CO)] (Figure 1).[21] Further details of this structure and a comparison to the further structures presented in this paper are shown below.

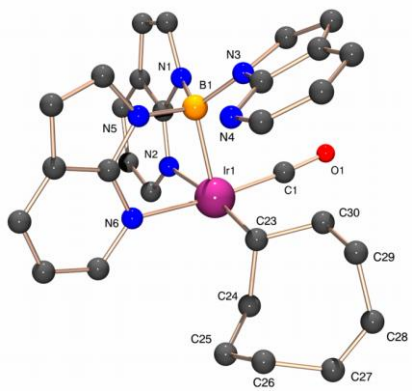

Figure 1 – Crystal structure of complex **6** (hydrogen atoms have been removed for clarity).

Confirming the location of the former borohydride species We had previously postulated that the incorporation of the hydrogen atom from the former borohydride moiety of the ligand into the cyclooctenyl group involved a transient iridium-hydride species.[10b] However, we were unable to obtain any spectroscopic evidence for this since the reaction proceeded too quickly. In order to provide further evidence concerning the endpoint location of the former borohydride hydrogen atom, a deuterium labeling study was carried out. The sodium salt of the deuterium labeled ligand, [B(D)(azaindolyl)$_3$]$^-$ (**Tai-d$_1$**) was prepared *via* an analogous route to that for K[**Tai**] (in this case, from $NaBD_4$ and four equivalents of 7-azaindole).[14a] The labeled complex, [Ir{κ^3-*NND*-B(D)(azaindolyl}$_3$(COD)] (**4-d$_1$**) was subsequently prepared also via an analogous route to that for **4** as outlined in Scheme 3. The B*D* resonance in **4-d$_1$** was located as a broad signal at 4.6 ppm in the ^{2}H-NMR spectrum (in C_6H_6). The slight upfield shift of this signal in comparison to free ligand [$\delta(CD_3CN)$ 5.9 ppm] is suggestive of some degree of interaction of the *BD* group with a d^8 center.

Scheme 3 – Synthesis of **4-d$_1$** from Na[**Tai-d$_1$**] and [IrCl(COD)]$_2$ and its subsequent reactivity with CO

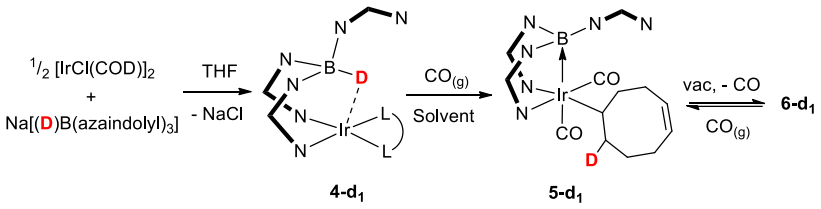

Complexes **5-d$_1$** and **6-d$_1$** were obtained *via* a similar manner to that described for **5** and **6** above. These two products (and additionally **5** and **6)**, were analyzed by a series of NMR experiments in order to assign the proton (deuterium) and carbon signal on the cyclooctenyl ring (Figure 2). Accordingly, the deuterium was located on the carbon β to the iridum center as expected. The two carbon nuclei bearing the deuterium substituents exhibited $^1J_{CD}$ coupling constants of 18.0 and 17.6 Hz for **5-d$_1$** and **6-d$_1$**, respectively. Additionally, ROESY NMR experiments carried out on **6-d$_1$** were consistent with addition of both hydrogen atom and metal center to the same side of the double bond, as expected.[22]

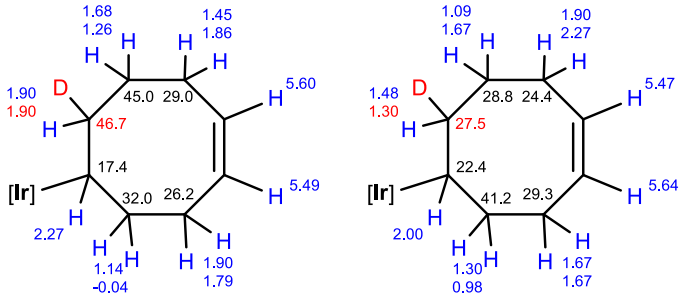

Figure 2 – Proton, deuterium and carbon NMR assignments (blue, red and black, respectively) for **5-d$_1$** (left) and **6-d$_1$** (right) in C_6D_6/C_6H_6. All other substituents at iridium have been removed for clarity.

Coordination properties of the site trans to boron The observation of the dicarbonyl product **5** in solution suggests that the site trans to Ir–B bond is available for coordination. It was possible to show that the coordination of carbon monoxide was reversible by NMR and IR spectroscopies (Scheme 2). The interconversion between **5** and **6** was confirmed by following the reaction coordinate by ^{11}B-NMR and IR spectroscopy. In a typical experiment, CO was bubbled through a toluene solution of **6**, and upon formation of a colorless solution, the IR and the ^{11}B-NMR (unlocked) spectra were collected and found to be identical to that described above. When the CO atmosphere was removed and replaced by N_2, complex **5** reverted to complex **6** again, shown by ^{11}B-NMR and IR spectroscopies.

The labile coordination of CO in the site trans to the boron atom demonstrates the highly unusual binding properties of this site. Since our original report, Connelly has provided a further example where the CO ligand can be readily removed from the coordination sphere of the complex (presumably the CO ligand is lost under reduced pressure during the work up procedure as found in the case of **5**).[8h] Furthermore, Hill[23] and Nakazawa[9a,b] have both reported cases where the CO ligand trans to boron undergoes reversible ligand substitution reactions with phosphines. Whilst a large number of metal-borane complexes containing a variety of ligands have now been reported, those featuring π-acceptor ligands such as carbon monoxide and isocyanides at the site trans to boron remain rare.[24] Amongst the examples now reported, there are many of which clearly highlight an enhanced trans labilization of the metal–ligand bond trans to the borane moiety. For example, in complexes **7** to **10** (Chart 3)[8d,25] which feature the same ligand both cis and trans to the borane ligand, the metal–ligand distances trans to boron are significantly elongated with respect to the one that is cis. Such elongation is more apparent in the square based systems compared to the trigonal bipyramidal based systems.[26] It was therefore of interest to gain further insight into the coordination potential of the site trans to boron in **6** and accordingly we subjected the complex to a variety of ligands (Scheme 4).

Chart 3 – Selected examples (**7** – **10**) demonstrating the enhanced labilization effect of the boron moiety (N═S' = 2-mercapto-1-^{t}butylimidazolyl, N═S = mt, R = 3,5 dimethylpyrazolyl).

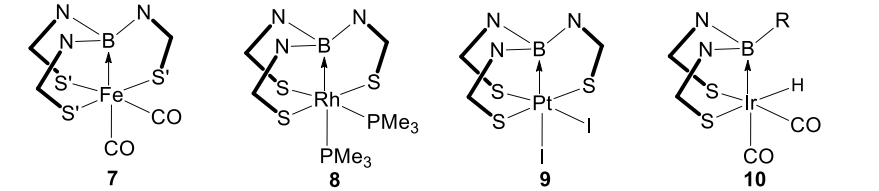

7 Fe-C_{cis} = 1.717(6) Å, Fe-C_{trans} = 1.800(6) Å

8 Rh-P_{cis} = 2.292(3) Å, Rh-P_{trans} = 2.471(3) Å

9 Pt-I_{cis} = 2.6497(3) Å, Pt-I_{trans} = 2.8787(3) Å

10 Ir-C_{cis} = 1.866(6) Å, Ir-C_{trans} = 1.980(6) Å

Further evidence to support the octahedral structure of complex **5** was obtained following the reaction of **6** with one equivalent of 2,6-dimethylphenyl isocyanide. One equivalent of the isocyanide ligand was added to a toluene-d_8 solution of **6** resulting in a color change from pale yellow to almost colorless. The $^{11}B\{^1H\}$ spectrum confirmed the formation of a new product, **11**, at 4.3 ppm (h.h.w. = 120 Hz), shifted

downfield from –9.3 ppm in the precursor to a similar region as that observed for **5** (5.8 ppm) (see Table 1). The ^{1}H NMR showed similar characteristics to that of complex **5** together with additional peaks corresponding to coordinated isocyanide. Complex **11** was synthesized on a preparative scale, in high yield and was fully characterized by NMR, IR spectroscopies, ESI^{+} mass spectrometry and elemental analysis.

Scheme 4 – Addition of π-acid ligands to complex **6**

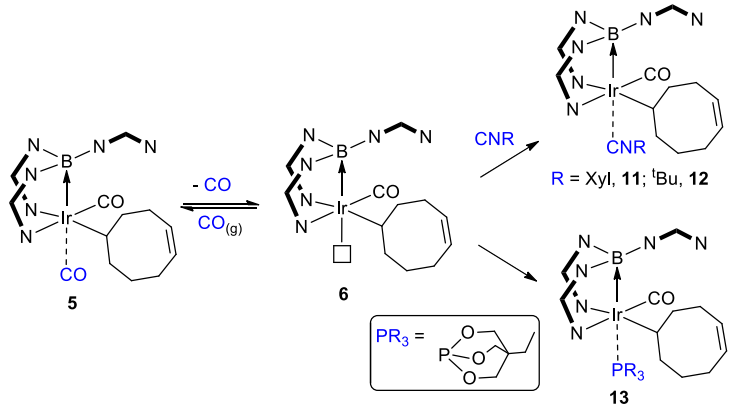

All of the evidence supported the formation of a complex containing both a carbon monoxide and an isocyanide ligand. Initially, the only uncertainty was in the position of these ligands with respect to the boron atom. The similarity of the ^{11}B-NMR shift of **11** with **5** suggests a geometry where the isocyanide ligand is positioned trans to the boron atom. A crystallographic study confirmed the position of the respective ligands. Single crystals were obtained by slow evaporation of pentane into a toluene solution of **11**. The crystal structure confirmed the formation of [Ir(C_8H_{13}){κ^3-*NNB*-B(azaindolyl)$_3$)(CO)(CNC_8H_9)] (**11**) and revealed that the isocyanide ligand indeed occupies the site trans to boron (Figure 3).

Table 1 – Selected NMR and IR spectroscopic data for complexes **5**, **6**, **11** – **13, 16** and **19**

Complex	Ligand trans to boron	^{11}B{^{1}H} shift[a]	h.h.w	Solution State (toluene) [b]

		δ (ppm)	(Hz)	CO / CNR (cm^{-1})
5	CO	5.8	42	2060, 2009 (2 × CO)
6	no ligand	−9.3	28	2008 (CO)
11	$CNC_6H_4Me_2$	4.3	119	2131 (CNR), 1987 (CO)
12	CN^tBu	3.7	121	2148 (CNR), 1994 (CO)
13	$P(OCH_2)_3CEt$	4.2[c,d]	–[d]	2013 (CO)[e]
16	CO	6.0	190	2061, 2010 (2 × CO)[f]
19	No ligand	–5.2	190	[g]

[a] toluene-d_8 unless otherwise stated; [b] as a toluene solution unless otherwise stated; [c] in CD_2Cl_2; [d] this signal appears as a doublet resonance as a result of $^2J_{PB}$ coupling (127 Hz); [e] neat; [f] tentatively assigned from the IR spectrum of the mixture of **16**, **17** and **18**; [g] not determined.

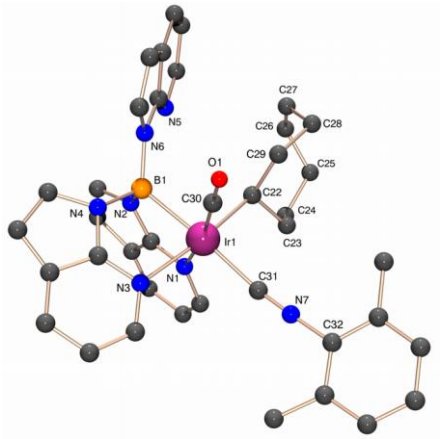

Figure 3 - Crystal structure of complex **11** (hydrogen atoms have been removed for clarity).

Further complexes were also targeted and the analogous complex [Ir(C_8H_{13}){κ^3-*NNB*-B(azaindolyl)$_3$)(CO)(CNC_4H_9)] (**12**) was also prepared by a similar reaction using ^{t}butyl isocyanide. Again complex **12** was fully characterized by spectroscopic and analytical methods (see experimental). The result of these tests confirm the coordinating ability of π-acids such as CO (**5**) and CNR (**11** and **12**) to the site trans to boron. In order to explore this further we treated complex **6** with one equivalent of $P(OCH_2)_3CEt$.[27] Ernst had previously described the low steric properties of this caged phosphite ligand describing it as a weak σ-donor and strong π-acceptor[28] and it was found to have a Tolman cone angle of 101°.[29] More recently, detailed computational investigations have been carried out probing the properties of this ligand in the context of the spectrum of monodentate phosphorus based ligands which

are consistent with the view that this ligand is among those P(III) ligands closest in properties to CO and CNR.[30] Addition of one equivalent of $P(OCH_2)_3CEt$ to a toluene-d_8 solution of **6** resulted in a color change from pale yellow to colorless and within a few minutes a white precipitate had formed. The product was isolated in high yield by removal of all volatiles and washing the resulting solid with pentane. The white solid was fully characterized by spectroscopic and analytical techniques and was consistent with the formation of [Ir(C_8H_{13}){κ^3-*NNB*-B(azaindolyl)$_3$)(CO){$P(OCH_2)_3CEt$}] (**13**). The $^{11}B\{^1H\}$ spectrum indicated the formation of a new product, **13**, at 4.2 ppm (d, $^2J_{PB}$ = 127 Hz). Again a similar chemical shift to the dicarbonyl product **6** (5.8 ppm) (Table 1). The $^{31}P\{^1H\}$ NMR spectrum of **13** was particularly broad suggesting its coordination to the site trans to the quadrupolar boron nuclei. A single broad resonance was observed at 97.8 ppm (h.h.w. = 429 Hz). The ^1H NMR showed similar characteristics to the complex **6** together with additional peaks corresponding to coordinated phosphite ligand. Complex **13** was synthesized on a preparative scale in high yield and was fully characterized by NMR, IR spectroscopies, ESI^+ mass spectrometry and elemental analysis. Single crystals were obtained by slow diffusion of pentane into a DCM solution of **13**. The structure confirmed the formation of [Ir(C_8H_{13}){κ^3-*NNB*-B(azaindolyl)$_3$)(CO){$P(OCH_2)_3CEt$}] (**13**) and revealed that the newly added phosphite ligand occupies the site trans to boron (Figure 4).

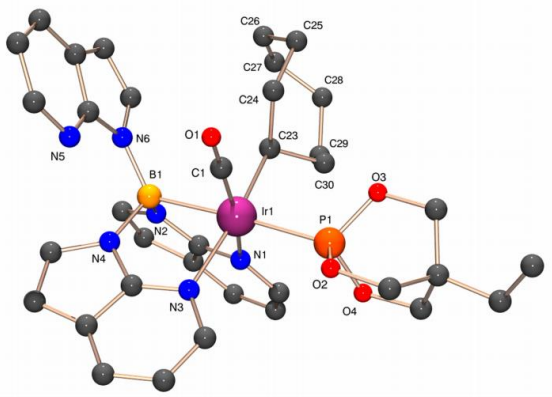

Figure 4 - Crystal structure of complex **13** (hydrogen atoms have been removed for clarity).

The coordination properties of complex **6** were further tested by the addition of other ligands. The strong σ-donor with a small Tolman angle, PMe_3 (118º),[29] was initially chosen to eliminate steric factors. One equivalent of PMe_3 was added to a solution of **6** in toluene. The $^{11}B\{^1H\}$ and $^{31}P\{^1H\}$

NMR spectra of the resulting mixture were recorded showing no signs of coordination of the phosphine after a period of 12 h. Similarly, other ligands such as pyridine, P^tBu_3 and the bidentate ligand dppe all failed to coordinate to the iridium center. Finally, no reactivity of **6** was observed with oxidants such as MeI or I_2. Based on these tests it appears that the site trans to boron shows a preference for π-acids.

Reactions involving hydrophenylbis(azaindolyl)borate, ^{Ph}Bai We have previously reported the synthesis and characterization of a new derivative ligand **^{Ph}Bai** [hydrophenylbis(azaindolyl)borate].[10c] It was possible to show that substitution of one azaindole ring with a phenyl group had a significant effect on the hydrogen migration properties of the resulting compound. As shown in Scheme 5, no hydrogen transfer into the rhodium bound NBD ligand was observed in the case of the **^{Ph}Bai** complex even at elevated temperatures (up to 100 °C). Here, the coordination of the third azaindole ring is important since it provides a stable square pyramidal product with a κ^4-*NNBN* coordination mode; this is not possible with the **^{Ph}Bai** ligand. For this reason, we were intrigued to test the reactivity of [Ir{κ^3-*NNH*-Ph(H)B(azaindolyl)$_2$}(COD)] (**15**)[10c] with carbon monoxide. In this case, it was originally envisaged that the 'third arm' of the ligand would be less important since it remains uncoordinated in both **5** and **6**. Accordingly, the reactivity of **15** was tested under the same conditions used for complex **4**.

Scheme 5 – The importance of the 'third arm' of the ligand in driving hydrogen migration into the norbornadiene ligand.

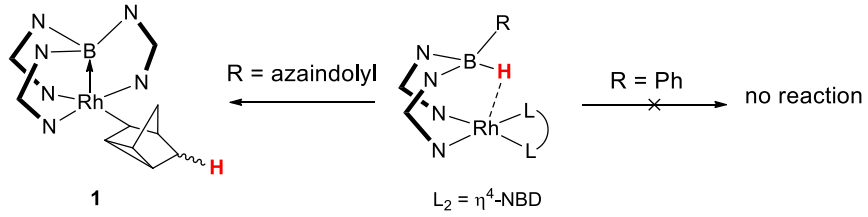

Complex **15** was dissolved in toluene-d_8 in a Young's NMR tube and was placed under a slight overpressure of CO (*ca*. 1.5 bar). The color of the solution changed from yellow to colorless over a period of 5 minutes. The $^{11}B\{^1H\}$ NMR spectrum of the mixture revealed the full consumption of the precursor. Two species were apparent in the spectrum, one major singlet peak at 6.0 ppm and a second one at 2.0 ppm. Both signals were relatively broad and overlapped with each other (see Figure S1 in

supporting information). The corresponding proton NMR spectrum revealed a more complex mixture of products. Even though the spectrum contained many signals, it was well resolved and three new iridium species (**16**, **17**, and **18**) could be distinguished in approximately 55%, 25% and 20% quantities (Scheme 6). The major species (**16**) was identified as [Ir(η^1-C_8H_{13}){κ^3-*NNB*-B(Ph)(azaindolyl)$_2$}(CO)$_2$] by direct comparison with the spectroscopic data for **5** [*c.f.* the $^{11}B\{^1H\}$ chemical shift of **16** (6.0 ppm) to that for **5** (5.8 ppm)]. Furthermore, a characteristic upfield signal at –0.25 ppm (similar to that observed in the ^1H NMR spectrum of **5**) was also apparent in the spectrum. Signals corresponding to the second product (**17**) were also identified. Here, the presence of a singlet resonance at –14.60 ppm revealed the formation of an iridium–hydride complex. A comparable amount of free 1,5-cyclooctadiene was also found in the spectrum, as determined by integration. Based on this evidence, species **17** was given the assignment, [I(H)r{κ^3-*NNB*-B(Ph)(azaindolyl)$_2$}(CO)$_2$]. Finally, the third iridium species (**18**) exhibited a number of broad multiplet signals (five signals were free from overlap with other signals in the spectrum) each integrating for one proton in the region 2.3 – 4.0 ppm. Further information concerning the identity of **18** was obtained in the corresponding $^{13}C\{^1H\}$ NMR spectrum. The spectrum confirmed that all eight signals of the cyclooctyl ring in **18** were located in the region between 15 ppm to 60 ppm. Three of these signals corresponded to carbons with only one hydrogen substituent. Accordingly, the chemical shifts of the olefinic carbon atoms were identified as those at 59.7 and 46.1 ppm. The high field chemical shift suggested that the double bond remains coordinated in **18**. Complex **18** was therefore given the tentative assignment, [Ir(σ^1,η^2-C_8H_{13}){κ^3-*NNB*-B(Ph)(azaindolyl)$_2$}(CO)].

Scheme 6 – Reactivity of complex **15** with CO

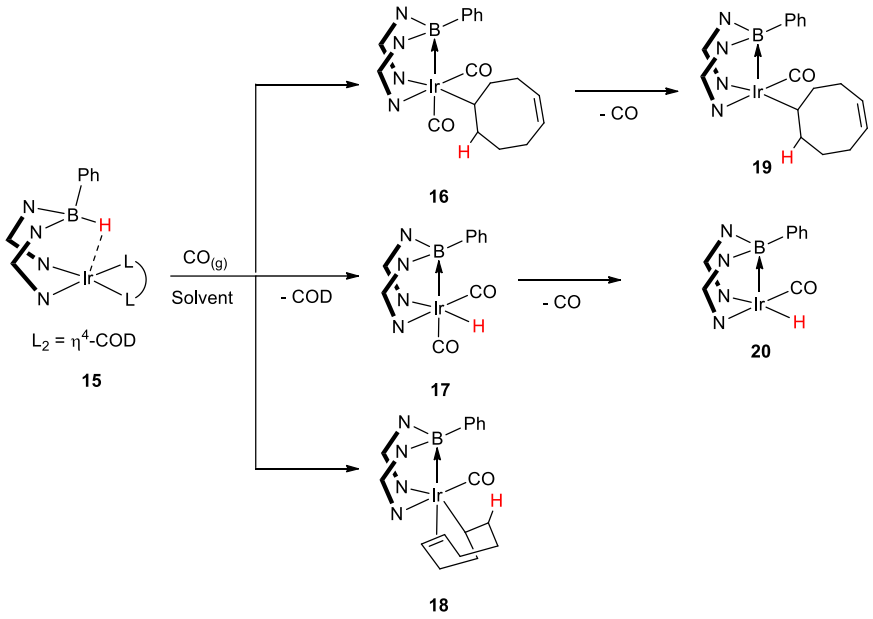

There were no significant changes in the distribution of complexes within the reaction mixture over time.[31] The mixture was therefore worked-up to see whether one or more of these species could be isolated. All volatiles were removed from the mixture and the residue extracted with pentane. A yellow solid precipitated from the solution after a period of 2 h at –80 °C. The resulting solid was analyzed by NMR spectroscopy. The spectra were similar to those found for complex **5** and were consistent with the formation of new complex [Ir(η^1-C_8H_{13}){κ^3-*NNB*-B(Ph)(azaindolyl)$_2$}(CO)] (**19**). Given our previous observations, it is very likely that **19** derives from the bis-carbonyl complex **16** via the analogous reactivity that was previously found between complexes **5** and **6** above (Scheme 6). It was possible to obtain a further species which was isolated from these mixtures when volume of the toluene solvent was reduced and pentane added. Single crystals of a new species [Ir(H){κ^3-*NNB*-B(Ph)(azaindolyl)$_2$}(CO)] (**20**) were obtained (Figure 5). Further details concerning this structure and its comparison to the other complexes described in this article are provided below. Again, complex **20** derives from **17** where the second carbonyl ligand is also lost upon work up (Scheme 6).

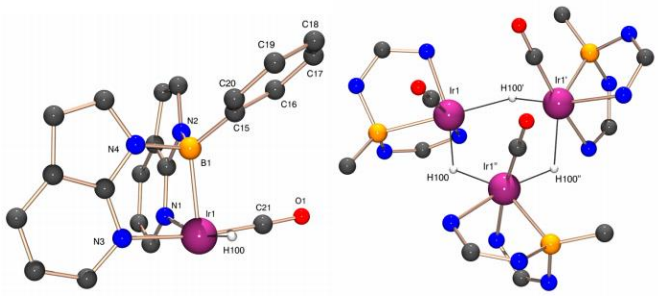

Figure 5 – Crystal structure of [Ir(H){κ^3-*NNB*-PhB(azaindolyl)$_2$}(CO)] (**20**) (left); the trimeric motif formed via the interaction of three Ir–H groups is on the right (in this case, only the structural core is shown for clarity). Selected bond distances (Å): Ir_1–H_{100} 1.71(3), $Ir_{1''}$–H_{100} 2.06(4), Ir•••Ir 3.2944(2).

A deuterium labeling investigation was also carried out exploring the reactivity of complex **15** with carbon monoxide in more detail. The deuterium labeled complex **15-d$_1$** was prepared via the same method as utilized for **15**. The reaction of **15-d$_1$** was monitored by $^{11}B\{^1H\}$ and ^1H NMR spectroscopy. As expected, a similar product distribution involving the components **16-d$_1$**, **17-d$_1$**, **18-d$_1$** and free COD was observed compared to the non-deuterium labeled reaction described above. The transfer of deuterium from boron to the iridium center was confirmed by the corresponding ^2H NMR spectrum in which a signal was observed at –14.5 ppm (**17-d$_1$**) along with signals at 1.7 ppm and 1.5 ppm. The latter two signals are likely to correspond to **16-d$_1$** and **18-d$_1$**.[32] Initially, the ^1H NMR spectrum indicated only a trace quantity of iridium–hydride species (at –14.5 ppm) however the relative integration of this signal was found to increase over time. It was evident in subsequent NMR spectra that a significant degree of protio/deuterio re-distribution was occurring over a period of a few days. A similar observation of deuterium scrambling upon a rhodium bound cyclooctyl ring has been reported.[8c]

Discussion

Spectroscopic Data A comparison of the selected NMR and IR spectroscopic data for complexes **5**, **6**, **11** – **13**, **16** and **19** are shown in Table 1. The effect of placing a ligand in the coordination site trans to the boron is of particular interest. Braunschweig recently completed a survey of the many different characteristics of metal-borane complexes including ^{11}B NMR chemical shifts.[4b] It was noted that ^{11}B

signals can be located over a broad range of chemical shifts (ca. 80 ppm to –10 ppm) and showed a strong dependence on the strength of the metal–borane dative bond. Those complexes in which the boron center feature two or three nitrogen substituents are found within a much smaller range and tend to contain significantly stronger dative bonds with shorter metal-boron distances. There have been no other reported examples where a previously empty coordination site trans to a borane group has been reacted further with additional ligands to furnish the complex with a higher coordination number. As shown in Table 1, the $^{11}B\{^{1}H\}$ NMR spectra show a marked change in the chemical shift of the boron nucleus upon coordination of a ligand to the sixth coordination site of the iridium center. The boron chemical shift changes from −9.3 ppm in the square based pyramidal complex **6** to 5.8 ppm in the octahedral complex **5** where a carbon monoxide ligand is coordinated trans to boron. This 15.1 ppm change in the chemical shift suggests a significant alteration in the electronic environment at the boron center. An analogous downfield shift is also observed in the **^{Ph}Bai** complexes **19** and **16** (Table 1). Furthermore, coordination of other ligands such as isocyanides and the phosphite ligand to **6** reveal similar downfield chemical shifts (c.f. 3.7 – 4.3 ppm for complexes **11** – **13**). Additionally, the nature of the ^{11}B signal changes from relatively sharp in **6** (hhw. = 26 Hz) to broad in the octahedral complexes (up to 121 Hz in complex **12**).[33] Connelly also observed a similar downfield change in chemical shift between the square based pyramidal complex $[Rh\{B(mt)_3\}PPh_3]$ and the octahedral complex $[Rh\{B(mt)_3\}PPh_3(CO)]$.[8h,34]

The carbonyl ligand is a very useful ligand to probe the electronic environment of the metal center.[35] Table 1 shows that the CO stretching frequencies of the mono-carbonyl complexes (and the CO ligand is cis to boron), are found in a small range (1987 to 2013 cm^{-1}) and do not significantly change. This value is within the range found for similar iridium(I) complexes.[36] Coordination of a second carbonyl ligand trans to boron in **5** results in two bands at 2060 cm^{-1} and 2009 cm^{-1}. An increase in the combined frequencies is perhaps expected by the addition of a further π-acceptor to the complex. Connelly has reported the iridium dicarbonyl hydride complexes **10** (Chart 3).[8d] In this complex, two carbonyl stretching frequencies were found at 2073 cm^{-1} and 2022 cm^{-1} in DCM solvent. In the case of the isocyanide complexes **11** and **12**, the carbonyl stretching frequencies are observed at 1987 cm^{-1} and

1994 cm^{-1}, respectively. These values are consistent with an increase in the σ-donor character of the isocyanides ligands allowing for further π-back donation into the cis carbonyl ligand.[37]

Structural comparison of complexes 6, **11**, **13** and **20** The iridium atom adopts a square based pyramidal geometry in **6** (Figure 1). The coordination sphere comprises of a coordinated molecule of carbon monoxide, a σ^1-bound cyclooctenyl group and a neutral B(azaindolyl)$_3$ ligand coordinated via two pyridyl nitrogen donors and the borane functional group (with a facial κ^3-*NBN* coordination mode). There is no ligand trans to the boron atom in complex **6**. The cyclooctyl group exhibits a pure σ^1-coordination mode, with no other significant interactions with the iridium center. While some σ^1-bound cyclooctenyl iridium complexes have been structurally characterized,[38,39] to our knowledge this is the first structurally characterized example coordinating solely *via* a Ir-C σ-bond (where the alkene functionality remains uncoordinated).[40] There does not appear to be any significant interactions between any of the hydrogen atoms on the cyclooctenyl ring, the closest iridium–hydrogen distance is 2.457 Å. This involves H_{24A}, which is attached to C_{24} and is β to the iridium center (Figure 1). As highlighted above, the ^{1}H NMR spectrum of **6** does not indicate any significant interaction between this or any other hydrogen atom on the cyclooctenyl ring. In this respect, it appears that the iridum center is stable as a pentacoordinate complex.

The iridium atom adopts an octahedral geometry in complexes **11** and **13** which are coordinated by the B(azaindolyl)$_3$ (with the same facial κ^3-*NBN* coordination mode found in **6**), one carbon monoxide, a σ^1-bound cyclooctenyl group and an isocyanide ligand for complex **11** or P(OCH$_2$)$_3$CEt ligand for **13** (Figures 3 and 4, respectively). In both cases, the isocyanide or phosphite ligands are situated trans to the boron center and the carbonyl ligands are sited cis to the boron center. There is a difference between the orientation of the cyclooctenyl ligand in complexes **11** and **13** when compared to that in **6**. The octenyl ring is orientated at a greater angle from the square plane [*c.f.* the B_1–Ir_1–C_α–C_β torsion angles 163.6(3) and –75.0(4) for **6** with –140.5(3) and 89.8(3) for **11**; –136.7(3) and 92.3(3) for **13**]. The empty site in **6** allows the cyclooctenyl group to extend down into the space below the square plane. In **11** and **13** this space is occupied by the sixth ligand. The octenyl groups in **11** and **13** move away from the metal center.

The iridium atom in **20** adopts a square based pyramidal geometry (Figure 5, left). The coordination sphere comprises of a coordinated molecule of carbon monoxide, a hydride ligand and a neutral B(Ph)(azaindolyl)$_2$ ligand coordinated via two of pyridyl nitrogen donors and the borane functional group. As found in **6** there is no coordinated ligand in the site trans to boron. In this case however, the complexes interact with each other in the solid state and form a trimeric structure with a Ir_3H_3 core (Figure 5, right). The iridium centers bridge via the hydride ligands with distances Ir_1–H_{100} 1.71(3) Å and $Ir_{1''}$–H_{100} 2.06(4) Å. The distances between the iridium centers is 3.2944(2) Å [c.f. $\sum_r$ (Ir–Ir) 2.82 Å].[41] A tetrametallic cluster featuring a Ir_4H_4 has recently been published.[42] There are also some examples of clusters featuring a Ir_3H_3 core,[43] which are capped by additional groups. The Ir–H–Ir bridges in **20** are much weaker than these literature examples however where the Ir–Ir distances are much shorter [typically in the region of the $\sum_r$ (Ir–Ir)]. This is perhaps expected since the mononuclear structure in **20** can already be thought of as "coordinatively saturated", as was found in the pentacoordinate complex **6** described above.

A comparison of all the important bond lengths and angles for complexes **6**, **11**, **13** and **20** is provided in Table 2. Accordingly to the X,L,Z classification,[3] complexes **6** and **20** (when considering the mononuclear structure) are of the type ML_3XZ, where Z is an σ-acceptor (in this case borane) and complexes **11** and **13** are of the type ML_4XZ. The difference between the two types of complex is one L-type ligand. The reversible coordination of the carbon monoxide (L) ligand to complex **6** suggests a low energy pathway between the ML_3XZ and ML_4XZ type complexes (the relative energies of **5** and **6** have been estimated by computational methods and are described below). The structural characterization of complexes **6**, **11**, and **13** allows a direct comparison to be made between the penta- and hexa-coordinate complexes. The Ir–B distance in **6** is 2.196(6) Å. Upon coordination of the isocyanide (in complex **11**), the iridium-boron distance increases 2.222(3) Å while in the case of the phosphite complex **13**, the iridium-boron distance increases to 2.240(4) Å (the distance is 2.245(5) Å in the second independent molecule within the structure). While these are only moderate increases, it does appear that the addition of a ligand in the site trans to boron destabilizes the dative interaction. This, at first, appears counterintuitive since the addition of a ligand which donates electron density through a σ-

donation should allow for an increase in the metal-to-boron dative interaction.[4b] While the isocyanide and phosphite ligands are known π-acceptors, the electron density taken back will be via orbitals not directly involved in the iridium-boron (if the borane function is considered only as a purely σ–donor). We recently reported the square planar (ML_3Z) and trigonal bipyramidal (ML_4Z) complexes, [Pd{κ^3-*SBS*-HB(mp)$_2$}(PPh$_3$)] (**21**) and [Pd{κ^4-*SBSS*-B(mp)$_3$}(PPh$_3$)] (**22**).[8a] Again, these complexes differ by the presence or absence of one donor ligand, L. In both complexes, the PPh_3 ligand is located trans to the borane and the new sulfur donor ligand (L) is added cis to the boron functionality. In contrast to the observations for complexes **6**, **11** and **13** above, the Pd–B distance is shorter in the complex containing the additional donor ligand [in **21** it is 2.091(3) Å while in **22** it is 2.065(3) Å]. The two ligand distances on the axial sites (Pd–B and Pd–P) of the trigonal bipyramidal complex **22** decrease, while the three Pd–S distances become significantly longer relative to those found in **21**. It appears that the geometry at the metal center has an important influence in the metal–boron bonding parameters.[4e] A further parameter which has been utilized as a means of estimating the strength of interaction between transition metals and borane moieties is the degree of pyramidalization of the boron center.[4c] In **6**, the sum of the three N–B–N angles at boron equals to 334.1°, showing a high degree of pyramidalization. The corresponding values for octahedral complexes are 327.0° for **11** and 326.8° and 327.9° for **13**. These latter values indicate the opposite trend, i.e. a higher degree of pyramidalization and a stronger metal–boron interaction, when compared to that in **6**; the higher degrees of pyramidalization in **11** and **13** suggesting enhanced interactions. There are a number of parameters which are involved in determining the strength of the interaction and the bond distance. The azaindole scaffolds are clearly very important since they impose some constraints. The fused bicyclic aromatic rings are planar and rigid. Nevertheless, flexibility can found in the Ir–N bond distances, the N–Ir–B–N torsion angles and the B–N bond distances. Indeed, the B–N distances differ quite significantly within the four complexes (the distances range between 1.518 Å to 1.567(4) Å) and are typically shorter in the five coordinate complexes.

Table 2 – Selected bond distances (Å) and angles (°) for complexes **6**, **11**, **13** and **20**.

Bond Distance/ Angle	**6**	**11**	**13** [a]	**20**
Ir–B	2.196(6)	2.222(3)	2.240(4) / 2.245(5)	2.248(3)
$Ir–N_{(trans\ to\ CO)}$	2.112(5)	2.111(2)	2.128(3) / 2.137(4)	2.124(2)
$Ir–N_{(trans\ to\ cyclooctenyl/H)}$	2.186(4)	2.188(3)	2.191(3) / 2.191(4)	2.149(2)
$Ir–C_{cyclooctenyl}$ or Ir–H	2.091(5)	2.146(3)	2.148(4) / 2.153(4)	1.71(3)
$B–N_{(trans\ to\ CO)}$	1.519(8)	1.558(7)	1.566(6) / 1.558(6)	1.552(4)
$B–N_{(trans\ to\ cyclooctenyl/H)}$	1.549(7)	1.567(4)	1.553(5) / 1.543(6)	1.556(4)
$B–N_{(free\ azaindolyl)}$ or $B–C_{Ph}$	1.518(7)	1.534(7)	1.525(6) / 1.527(7)	1.592(4)
Ir–CO	1.826(6)	1.841(3)	1.841(4) / 1.833(4)	1.828(3)
$Ir–L_{trans}$ [CNR or $P(OR)_3$]	–	2.083(3)	2.354(1) / 2.3570(11)	–
IrC≡O	1.146(7)	1.141(4)	1.145(5) / 1.148(5)	1.151(3)
N–Ir–N	88.26(16)	85.68(9)	90.28(13) / 90.78(15)	90.17(8)
$N–Ir–C_{CO}$ [b]	93.5(2)	94.85(12)	92.48(15) / 91.80(15)	89.51(10)
$N–Ir–C_{cyclooctenyl}$ or N–Ir–H [b]	87.55(19)	84.59(10)	82.82(15) / 83.04(17)	92.5(10)
$C_{CO}–Ir–C_{cyclooctenyl}$ or C_{CO}–Ir–H	91.4(2)	93.43(12)	92.65(17) / 92.61(17)	86.0(10)
$B–Ir–C_{CO}$	89.4(2)	87.6(2)	87.98(16) / 87.80(17)	89.29(11)
$B–Ir–C_{cyclooctenyl}$ or B–Ir–H	104.6(6)	91.35(13)	89.40(15) / 90.26(18)	85.8(10)
$B–Ir–N_{(trans\ to\ CO)}$	83.7(2)	82.09(19)	81.13(15) / 80.17(17)	82.72(9)
$B–Ir–N_{(trans\ to\ cyclooctenyl/H)}$	80.42(19)	80.38(13)	81.11(14) / 81.18(17)	81.18(10)
$\sum$of the N–B–N and N–B–C angles	334.1	326.97	326.8 / 327.9	331.5
$N–Ir–B–N_{(trans\ to\ cyclooctenyl/H)}$	–18.8(3)	17.9(3)	5.5(2) / –4.7(3)	–16.58(15)
$N–Ir–B–N_{(trans\ to\ CO)}$	7.6(3)	–7.0(2)	–14.4(2) / 15.6(3)	3.88(15)

[a] – there are two independent complexes in the asymmetric unit of complex **13**. The corresponding bond distances and angles of the second complex are also provided in the table as the second values; [b] – the angle provided involves the groups which are mutually trans to each other.

The structures **6**, **11**, **12**, and **20** all exhibit some distortion from their idealized square based pyramidal or octahedral geometries. The borane functionality occupies the axial site in the square based pyramidal complexes (**6** and **20**) and in all complexes the N–Ir–B angles are significantly smaller than

the idealized 90° angle [the N–Ir–B angles in the complexes range between 80.38(13)° and 83.7(2)°]. In all cases, the N–Ir–B angle is the one which has the greatest deviation from the idealized angle, with the exception of B–Ir–$C_{cyclooctenyl}$ angle in **6** [104.6(6)°]. As highlighted in Chart 3, the boron group imposes a significant trans labilization over the ligand in the site trans to it. Indeed, the Ir–C(31) distance (isocyanide trans to boron) in **11** is 2.083(3) Å. This is one of the largest Ir–CNR distances reported in the literature.[44] In the case of complex **13**, the Ir–P(1) distances are 2.354(1) Å and 2.3570(11) Å (for the two independent molecules in the same structure). Again, these distances are longer than any other structurally characterized iridium-phosphite complex reported in the literature, with the exception of one complex.[45]

Mechanism involved in the formation of σ^1–cyclooctenyl complexes

We had previously postulated a reaction pathway involved in the formation of **5** and **6** in our initial communication.[10b] Herein, we report the results of our density functional theory investigations which explore the mechanisms involved in this transformation in detail. The calculations used the B3PW91 functional, and an approximate correction for dispersion effects is included. The transformation involving the loss of the cyclooctadiene ligand in the reaction of complex **15** with CO is also discussed. The deuterium labeling studies presented above confirm the final position of the former borohydride hydrogen atom as the β-position of the cyclooctenyl group. The transfer of this hydrogen atom proceed either via a metal assisted process, involving an intermediate iridium–hydride species or via a non-metal assisted mechanism resulting from direct transfer of the hydrogen from the boron to the organic moiety. The fluxional behavior[14c] and various coordination modes of **Tai** (i.e. κ^2-*NH*, κ^2-*NN*, κ^3-*NNH* and κ^3-*NNN*)[14] have previously been noted. As a result, there are many feasible pathways to complexes **5** and **6** involving the aforementioned changes of the ligand scaffold, and the situation can become more complicated taking into account the possible alterations in the coordination mode of COD from η^4 to η^2. All possible mechanisms were explored computationally in order to verify the correct mechanism. Two principal routes to **5** and **6** are shown in Figure 6. This involves either the metal assisted mechanism (species **4ii** to complex **6** *via* **4iii**) or the non-metal assisted pathway (directly from **4ii** to **6**).

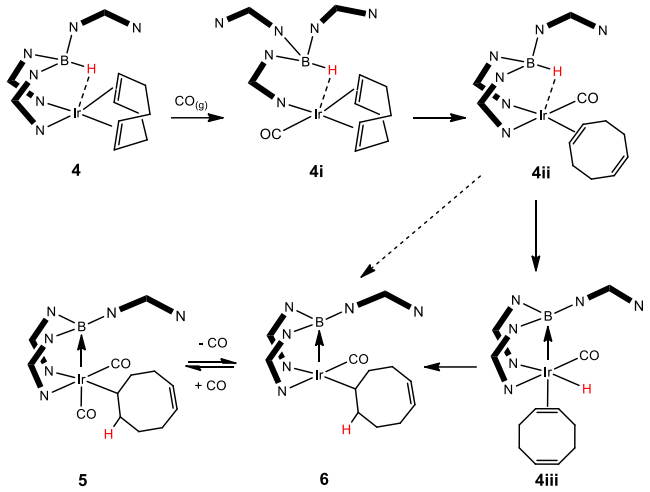

Figure 6 – Possible mechanisms for hydrogen transfer from boron to the cyclooctadiene unit triggered by addition of CO. The possible pathway where **4ii** is formed directly from **4** was also calculated and was found to have a slightly higher energy barrier than the one shown in the figure (see text for further details).

The computed structure $\mathbf{4_{calc}}$ was in excellent agreement with the crystal structure **4**.[14c] Further details in addition to selected bond lengths (Å), angles and torsion angles (º) for $\mathbf{4_{calc}}$ and all other calculated complexes described herein are provided in Table S1 of the supporting information. As shown in Figure 6, reaction of **4** with CO results in either the displacement of one of the azaindolyl rings from the coordination sphere or one of the double bonds of COD ligand, to form **4i** or **4ii**, respectively. The relative energies of these species have been calculated and are shown in Figure 7. The energies of both structures are lower than $\mathbf{4_{calc}}$, though the free energy of $\mathbf{4ii_{calc}}$ (which involves a κ^3-*NNH* coordination mode for **Tai** and a η^2-COD coordination mode for COD) is lower in energy by 9.9 kcal mol^{-1}, presumably due to the greater freedom associated with the η^2 coordinated eight-membered ring. The potential intermediate species, $\mathbf{4i^{-CO}_{calc}}$ and $\mathbf{4ii^{-CO}_{calc}}$ (Figure 8), which provide dissociative routes to complexes **4i** and **4ii** were also calculated.[46] These two intermediates are formed by either changing the coordination mode of the **Tai** from κ^3-*NNH* to κ^2-*NH* ($\mathbf{4i^{-CO}_{calc}}$) or changing the coordination mode of COD ligand from η^4 to η^2 ($\mathbf{4ii^{-CO}_{calc}}$) as indicated in Figure 8. The calculations reveal that a change in the coordination mode of the COD requires a significant amount of energy (44.3 kcal mol^{-1}). This is perhaps expected since the structure of $\mathbf{4ii^{-CO}_{calc}}$, as shown, deviates significantly from the preferred

square planar geometry of the iridium(I) center. Furthermore the **Tai** ligand is unable to accommodate a meridial κ^3-*NNH* coordination mode. Accordingly, the structure **4ii**$^{-CO}_{calc}$ is significantly higher in energy than dissociation of one of the azaindolyl rings from the coordination sphere. The optimised structure of **4i**$^{-CO}_{calc}$ reveals that 15.3 kcal mol^{-1} is required to change the coordination mode from κ^3-*NNH* to κ^2-*NH*. While this requires less energy, Figure 8 highlights the fact that significant structural rearrangement is required to form this intermediate. For these reasons it is highly likely that a concerted mechanism, involving simultaneous addition of CO and change in coordination mode of **Tai**, is involved in the formation of **4i**. A similar process involving a κ^3-*NNH* to κ^2-*NH* change in coordination mode was observed experimentally by Saito *et al.* upon addition of CO to [Ru(Cp*)**Tai**] [where Cp* = $C_5(CH_3)_3$].[14b]

The transformation of between **4i** and **4ii** requires an isomerisation process to occur. We have previously demonstrated that in complex **4**, the uncoordinated azaindolyl unit undergoes exchange with the coordinated azaindolyl units at ambient temperatures.[14c] For the transformation to **4ii** it is likely that one of the uncoordinated azaindolyl units in **4i** rotates and carries out an intramolecular substitution reaction thus assisting in the change in coordination mode of the COD ligand (i.e. η^4 to η^2). In free energy terms the isomerisation process, from **4i** to **4ii**, is favorable by 9.9 kcal mol^{-1}). Species **4ii** is the intermediate which will lead to the productive formation of complexes **5** and **6**.

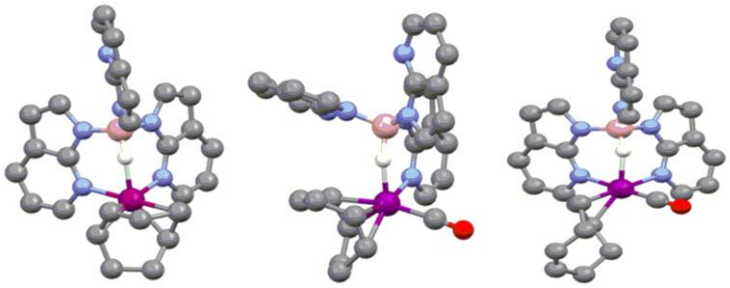

	4$_{calc}$	**4i**$_{calc}$	**4ii**$_{calc}$
ΔE_{rel} (kcal mol^{-1})	0.0	-16.4	-14.8
ΔG_{298} (kcal mol^{-1})	0.0	-6.1	-16.0

Figure 7 – Calculated structures of **4**$_{calc}$, **4i**$_{calc}$ and **4ii**$_{calc}$. Energies are relative to **4**$_{calc}$ and given in kcal mol^{-1}. All hydrogen atoms (except migrating hydrogen) have been omitted for clarity.

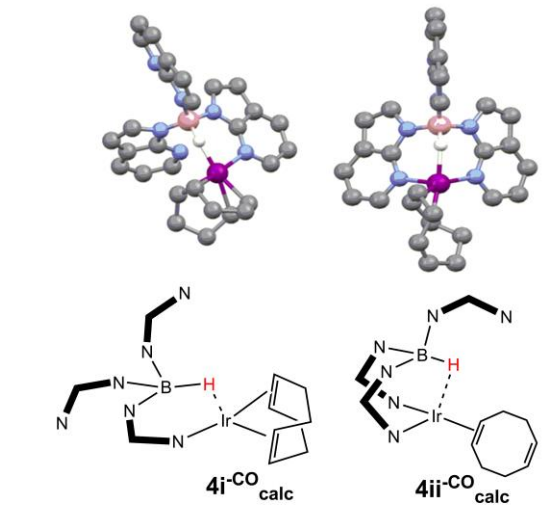

Figure 8 – Possible intermediate species **4i**$^{-CO}_{calc}$ and **4ii**$^{-CO}_{calc}$ resulting from the dissociative pathways. Energies are relative to **4**$_{calc}$ and are given in kcal mol^{-1}. All hydrogen atoms (except migrating hydrogen) have been omitted for clarity.

The step involving migration of hydrogen between boron to iridium centers

Having established the most likely route to **4ii**, the next step in our calculations was an exploration of the step involving hydrogen migration from boron. Firstly, the possibility of direct transfer to the cyclooctadiene unit was studied. In this case the hydrogen would migrate to the organic unit without forming an intermediate iridium-hydride species. Attempts were made to locate a transition state for such a migration, but despite multiple searches, no structure of this type could be found with an energy low enough to be competitive with the pathway involving an iridium–hydride species. Accordingly, this mechanism was ruled out. Based on these observations, the most likely route to **6** is via an iridium–hydride species. Furthermore, the formation of iridium–hydride complexes from borohydride precursors indeed has literature precedent.[8c,d,i,47] From **4ii**, the hydrogen atom migrates from the boron to the iridium, forming an octahedral complex with the formula [Ir(H){κ^3-*NBN*-B(azaindolyl)$_3$}(η^2-COD)(CO)]. There are three potential isomers of this newly formed complex where the three ligands (hydride, carbonyl and olefin) occupy different positions with respect to each other. The relative energies of the three isomers were calculated (see electronic supporting information for details) and it was found that the most stable isomer is the one presented as **4iii** (Figure 6), where the hydride and

carbonyl ligands occupy sites cis with respect to the boron and the olefin occupies the site trans to the boron. In this case, the migration of the hydrogen 'pushes' the COD ligand to the site trans to the boron. The trans influence of the boron functionality is immediately apparent here with a significant increase in the distance between the iridium center and the centroid of the C=C bond in the olefin. In **4iii$_{calc}$** the distance was calculated to be 2.31 Å, while in **4ii$_{calc}$** it is 2.00 Å; the latter distance is more typical of those found in the literature. The lowest energy conformation for **Tai** (in structure **4iii$_{calc}$**) is where the uncoordinated azaindole arm is rotated through 74.8º, the torsion angle Ir-B-N-C changes from 179.1º in **4ii$_{calc}$** to -73.9º in **4iii$_{calc}$**.

There has been much discussion regarding the reversible nature of hydrogen atom migration between borohydride units and metal centers (Scheme 1).[4a,48] The synthesis of the complexes [Ir(**H**){*o*-($Ph_2PC_6H_4$)$_2$(Ph)B}(CO)(PPh_3)] and [Rh{*o*-($Ph_2PC_6H_4$)$_2$(Ph)B**H**}(CO)(PPh_3)], has very recently been reported.[9h] The position of the hydrogen atom in these related group nine complexes is different (as highlighted in bold). Nakazawa and Kameo calculated the energies of these two compounds along with the corresponding complexes where the position of the hydrogen atoms is reversed. They found that [Rh(**H**){*o*-($Ph_2PC_6H_4$)$_2$(Ph)B}(CO)(PPh_3)] and [Ir{*o*-($Ph_2PC_6H_4$)$_2$(Ph)B**H**}(CO)(PPh_3)] were 8.0 kcal mol^{-1} and 2.4 kcal mol^{-1} higher in energy than their respective isomers. These theoretical studies are certainly consistent with literature observations.[4a] To our knowledge, however, there have been no computational investigations looking at energy profile of the hydrogen migration process. In free energy terms, the calculated structure of the hydrogen migration product **4iii$_{calc}$** was found to be 19.4 kcal mol^{-1} lower in energy than the starting complex **4$_{calc}$** meaning that the iridium−hydride species (**4iii$_{calc}$**) is more stable than the borohydride species (**4ii$_{calc}$**) by 3.4 kcal mol^{-1} (Figure 9). In order to gain more insight into this process, the transition state connecting **4ii$_{calc}$** and **4iii$_{calc}$** was calculated (Figures 9 and 10). The transition state, **TS$_1$** clearly shows the hydrogen at an intermediate point between the boron and iridium centers with elongated distances, B•••H = 1.68 Å, Ir•••B = 2.41 Å and Ir•••H = 1.63 Å. Similar distances B•••H and Ru•••H were found in the structurally characterized complex **3** (Chart 2) which features a situation where the hydrogen atom is "locked" between the two centers (the position of the hydrogen atom in **3** was also supported by DFT calculations).[13] The Ir•••B distance in **TS$_1$** is at an

intermediate value between those found in **4ii$_{calc}$** (2.96 Å) and **4iii$_{calc}$** (2.21 Å).[49] The B−Ir−H angle changes from 17.0 º to 44.3 º to 82.0 º upon going from **4ii$_{calc}$** to **TS$_1$** to **4iii$_{calc}$**. In free energy terms, the energy required to reach **TS$_1$** from **4ii$_{calc}$** was calculated to be 10.3 kcal mol^{-1} and from **4iii$_{calc}$** to **TS$_1$** (the reverse) it was found to be 11.6 kcal mol^{-1}. The corresponding potential energy values are 9.7 kcal mol^{-1} in the forward direction and 12.4 kcal mol^{-1} in the backwards direction. Given the relatively small activation barriers to the transition state between **4ii** and **4iii** and the small energy difference between the two species, it is reasonable to assume that the reversible hydride migration is energetically feasible. This clearly has implications for potential future applications where the reactivity outlined in Scheme 1 is desired.

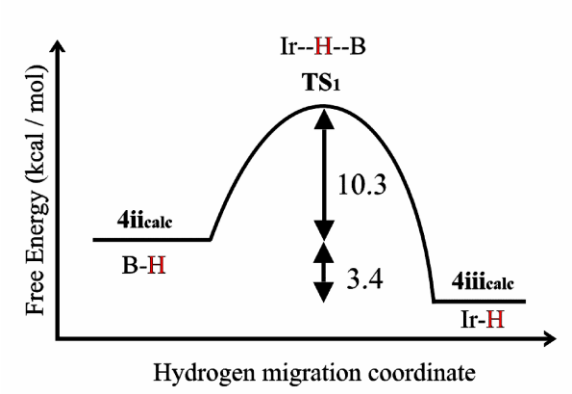

Figure 9 – The hydrogen migration coordinate between **4ii** and **4iii**

The next step in the reaction involves the migratory insertion of the COD ligand into the newly formed iridium–hydride species. Figure 10 also shows the transition state, **TS$_2$**, to this insertion reaction. In the transition state, the double bond moves towards the site cis to the borane ligand where the B–Ir–C=C$_{(centroid)}$ angle is 145.8°. The insertion results in the formation of a direct Ir–C bond and the hydrogen atom undergoes migration from the iridium center to the β-carbon. The product of this reaction step is **6**. The calculated structure, **6$_{calc}$**, agrees very well with the crystal structure **6** described above (see supporting information). This transition state reveals an elongated iridium–hydride distance (1.71 Å) and a largely formed C$_β$–H bond (1.36 Å). In potential energy terms, the barrier to the transition state was calculated to be 21.8 kcal mol^{-1} for the migratory insertion step and 33.0 kcal mol^{-1} for the corresponding β-hydride elimination step. In free energy terms the forward barrier for this step is

21.1 kcal mol^{-1} and the reverse is 32.0 kcal mol^{-1}. Accordingly, the overall migratory insertion step is energetically favorable by 10.9 kcal mol^{-1} (using the free energy values). The free energy activation barrier for **TS$_2$** is by far the largest of the two transition states involving the hydrogen migration and migratory insertion steps (c.f. 21.1 kcal mol^{-1} for **TS$_2$** and 10.3 kcal mol^{-1} for **TS$_1$**). Despite this, the migratory insertion step provides a strong driving force for the hydride migration step. The free energy calculated structure **6$_{cal}$** is 30.3 kcal mol^{-1} lower in energy than the starting complex **4$_{calc}$**. These values are consistent with our experimental observations in which the transformation of **4** to **6** occurs within approximately 10 min.

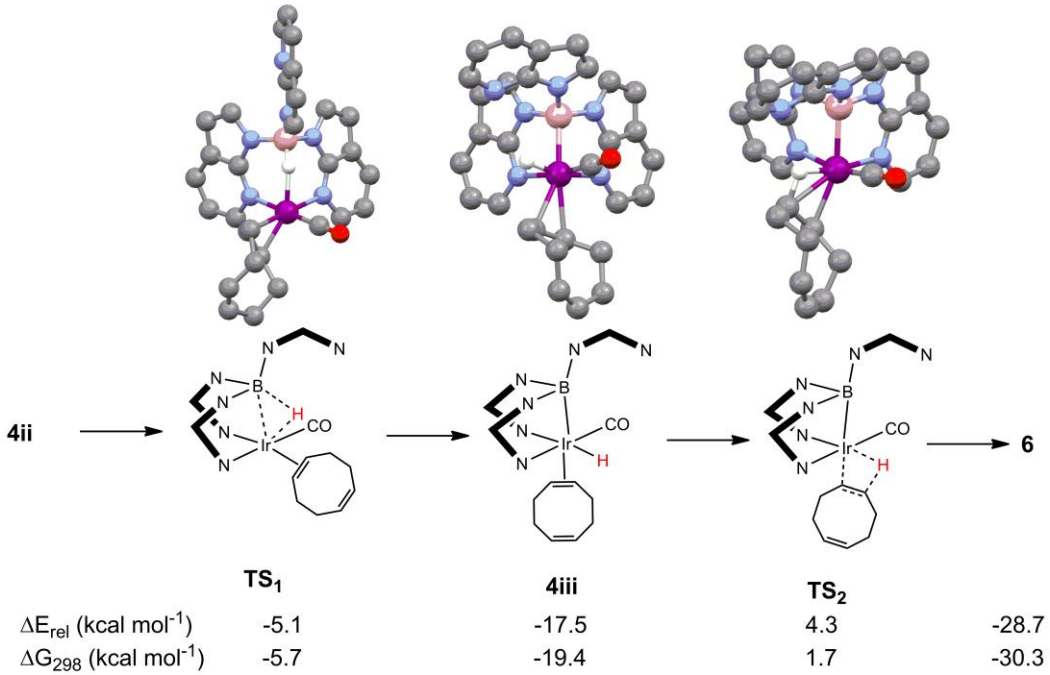

Figure 10 – Calculated geometries and schematic diagrams for **TS$_1$, 4iii** and **TS$_2$**. Energy relative to **4$_{calc}$** and given in kcal mol^{-1}. All hydrogen atoms (except migrating hydrogen) have been omitted for clarity.

The energy of complex **5**, where a second carbonyl ligand occupies the coordination site trans to boron, was calculated in order to obtain a greater understanding of these complexes (details are provided in the electronic supporting information). The complex was found to be 24.4 kcal mol^{-1} lower in energy terms than complex **6** (53.1 kcal mol^{-1} lower in energy than **4**, see electronic supporting information). On the other hand, the calculated free energy for binding CO is smaller by 11.9 kcal mol^{-1} due to the large negative change in entropy incurred upon ligand binding. Hence, while the calculated bond energy

is on the large side, it remains consistent with the experimentally observed situation, whereby **6** is formed in the presence of small partial pressures of carbon monoxide, but **5** is observed in absence of CO. It clearly demonstrates the interesting coordination properties of the site. The case is more intriguing when considering complex **10** reported by Connelly (Chart 3). Complex **10** shares quite similar characteristics to those of the calculated structure $\mathbf{5_{calc}}$, most specifically the Ir–CO bond distances. In $\mathbf{5_{calc}}$, the cis and trans (relative to boron) Ir–CO distances are 1.86 Å and 1.98 Å, while in **10** they are 1.866(6) Å and 1.980(6) Å, respectively. Whilst the CO trans to boron is not lost upon work-up in **10**, Connelly did show that the ligand could be substituted by triphenylphosphine.[8d] For these reasons, we are unable to explain with any degree of confidence why the carbonyl ligand is eliminated from the coordination sphere during our work-up involving complex **6** and not in the case of the literature compound **10**. The unusual coordination properties of the site trans to boron are also apparent in the reaction of ^{Ph}**Bai** complex **14** with CO. As described above, a mixture of products is obtained one of which is complex **20** where the COD ligand is eliminated from the complex before the migratory step can occur. This might be explained by the trans influence of boron found in $\mathbf{4iii_{calc}}$ where the Ir–olefin bond was found to be significantly elongated (2.31 Å) and the relatively high barrier to migration insertion. Presumably, these factors become more important in the complexes containing the ^{Ph}**Bai** ligand. While this might explain why the expected cyclooctenyl complexes **16** and **19** are not exclusively formed in this case, we are at present unable to explain the selectivity for σ^1,η^2-cyclooctenyl complex **18**. This is apart from the fact that this coordination mode is well known for the cyclooctenyl ligand, while the σ^1 coordination mode is not.[38,39] Figure 11 shows the potential energy surface along the reaction coordinate from complex **4** to complex **6**. It highlights a strong driving force to the formation of complexes **6** and **5** via relatively low energy transition states, in particular the migration of hydrogen from boron to metal center.

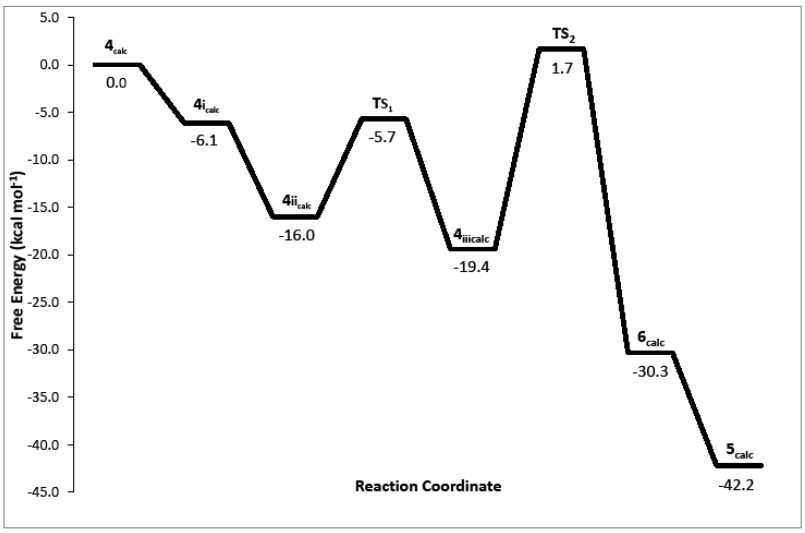

Figure 11 – The free energy surface along the reaction coordinate from complex **4** to complex **6** (**4_{calc}** = [Ir{κ^3-*NNH*-BH(azaindolyl)$_3$}(η^4-COD)], **$4i_{calc}$** = [Ir{κ^2-*NH*-BH(azaindolyl)$_3$}(η^4-COD)(CO)], **$4ii_{calc}$** = [Ir{κ^3-*NNH*-BH(azaindolyl)$_3$}(η^2-COD)(CO)], **TS_1** = hydrogen migration step, **$4iii_{calc}$** = [Ir(H){κ^3-*NNB*-B(azaindolyl)$_3$}(η^2-COD)(CO)], **TS_2** = migration insertion step, **6_{calc}** = [Ir(σ^1-COE){κ^3-*NNB*-B(azaindolyl)$_3$}(CO)] and 5_{calc} = [Ir(σ^1-COE){κ^3-*NNB*-B(azaindolyl)$_3$}(CO)$_2$]).

Conclusions

In this study we have explored the reactivity of flexible scorpionate ligands, **Tai** and **^{Ph}Bai**. These ligands have been shown to adopt a wide variety of coordination modes, κ^2-*NH*, κ^3-*NNH* and κ^3-*NNB*. We have demonstrated their potential to act as sources of 'hydride' where the hydrogen atom is transferred to the metal center and can undergo subsequent incorporation into an organic fragment. This is the first reported case where the **^{Ph}Bai** ligand has displayed such reactivity.

The mechanism for hydrogen atom transfer from the borohydride function to the former COD moiety has been modeled computationally and is consistent with both the experimental evidence and our original postulations. The hydrogen migration reactivity is triggered by carbon monoxide which first disturbs the coordination sphere, the hydrogen undergoes facile migration to the iridium center to form a transient iridium–hydride species. The computational studies outlined herein support the fact that

hydrogen atom migration from boron to metal as shown in Scheme 1 is a low energy process. For the complex containing the **Tai** ligand, the cyclooctadiene unit undergoes migratory insertion into the metal-hydride to form the new complex **5**. For the ^{Ph}**Bai** system, a similar reactivity is observed along with other transformations in which the diene is eliminated from the complex to form complexes **17** and **20**. The trans influence of the boron and the rate of migratory insertion are likely to be important factors in determining the product selectivity.

The unusual characteristics of these metal–borane complexes were explored. Even though complex **5** was stable under ambient conditions it was possible to expand its coordination number (from a ML_3XZ type complex to ML_4XZ). It was found that ligands such as carbonyl, isocyanides and phosphites were all successfully added to the coordination site trans to the boron. The resulting complexes contained elongated metal–ligand bond distances. In contrast, donor ligands such as alkyl phosphines and pyridine failed to add to this site.

Experimental

General considerations: All manipulations were performed in a Braun glovebox with an O_2 and H_2O atmosphere of below 5 ppm or by using standard Schlenk techniques. [Ir(**Tai**)(COD)][14c] and [Ir(^{Ph}**Bai**)(COD)][10c] were prepared according to a published procedures. The solvents toluene, THF and Et_2O were dried using a Grubbs' alumina system, dry n-pentane (< 0.05 ppm H_2O) was purchased from Fluka and DCM was dried over CaH_2. All solvents were subsequently kept in Young's ampoules under N_2 over activated molecular sieves (4 Å). Deuterated toluene and benzene were degassed by three freeze-thaw cycles, dried by refluxing over sodium for 12 h, and kept in a Young's ampoule over 4 Å molecular sieves under N_2. ^{1}H-NMR, ^{11}B{^{1}H}-NMR, ^{11}B-NMR and DEPT-135 spectra were recorded on a JEOL ECP300 spectrometer operating at 300 MHz (^{1}H). ^{13}C{^{1}H}-NMR and correlation experiments spectra were recorded on a Varian VNMR S500 operating at 500 MHz (^{1}H). The spectra were referenced internally, to the residual protic solvent (^{1}H) or the signals of the solvent (^{13}C). ^{11}B{^{1}H}-NMR and ^{11}B-NMR spectra were referenced externally relative to $BF_3{\cdot}OEt_2$. Mass spectra were recorded on a VG Analytic Quattro in ESI^+ mode. Elemental analyses were performed at the microanalytical laboratory of the School of Chemistry at the University of Bristol. Infrared spectra were

recorded on a Perkin-Elmer Spectrum One FT-IR spectrometer (solution, NaCl cell) or a Perkin-Elmer Spectrum 100 FTIR spectrometer (solid state, neat) from 4000 cm^{-1} to 650 cm^{-1}.

[Ir(C_8H_{13}){κ^3-*NNB*-B(azaindolyl)$_3$}(CO)$_2$] (5)

A sample of [Ir(**Tai**)(COD)] (25 mg, 0.038 mmol) was placed in a Young's NMR tube and dissolved ca. 0.6 mL of d^8-toluene. The tube was connected to a vacuum line and the inert atmosphere removed by two freeze-thaw cycles. The solution was allowed to equilibrate at RT and the NMR tube was connected to a CO cylinder and pressurized to ca. 1.5 bar. This mixture was vigorously shaken under the dynamic positive pressure. After a few minutes the color of the solution changed to almost colorless and the NMR tube was removed from the CO supply. The spectroscopic data of the solution revealed **5** as the only observable species. NMR, δ($C_5D_5CD_3$): ^{1}H (300 MHz), 8.16 (1H, dd, $^4J_{HH}$ = 1.5 Hz, $^3J_{HH}$ = 4.4 Hz, aza), 7.83 (1H, dd, $^4J_{HH}$ = 1.5 Hz, $^3J_{HH}$ = 4.4 Hz, aza), 7.76 (2H, m, aza), 7.72 (1H, d, $^3J_{HH}$ = 3.7 Hz, aza), 7.41 (1H, d, $^3J_{HH}$= 3.7 Hz, aza), 7.15 (1H, $^3J_{HH}$ = 2.9 Hz, aza), 7.13 (2H, dd, $^4J_{HH}$ = 1.5 Hz, $^3J_{HH}$ = 7.3 Hz aza), 6.81 (1H, m, aza), 6.62 (1H, d, $^3J_{HH}$ = 2.9 Hz, aza), 6.36 (2H, 2 overlapping d, $^3J_{HH}$ = 2.9 Hz, aza), 6.26 (2H, m, aza), 5.46 (2H, m, C*H*=C*H*), 2.21 (1H, broad, C_8H_{13}), 1.86 (2H, m, C_8H_{13}), 1.75 (2H, m, C_8H_{13}), 1.60 (1H, m, C_8H_{13}), 1.41 (1H, broad s, C_8H_{13}), 1.15 (3H, m, C_8H_{13} including Ir-C*H*), -0.07 (1H, broad s, β-hydrogen, IrC_8H_{13}); ^{13}C{^{1}H} (125 MHz), 179.1 (s, *C*O), 170.0 (s, *C*O), 156.8, 156.5, 152.5, 142.7, 142.4, 142.2, 132.4, 131.1, 130.8, 130.4, 129.8, 128.9, 128.8, 127.4, 123.4, 121.7, 121.4, 115.5, 115.4, 115.3, 104.2, 103.5, 101.3 (azaindole and *C*H=*C*H), 46.2, 44.6, 31.6, 28.7, 25.7 (*C*H$_2$'s of cyclooctenyl), 17.0 (Ir-*C*H); ^{11}B{^{1}H}, 5.83 (s, $\Delta\nu_{1/2}$ = 42.1 Hz); ^{11}B, 5.83 (s); IR (toluene): 2060 cm^{-1}, 2009 cm^{-1} ν(CO); IR (THF): 2060 cm^{-1}, 2012 cm^{-1} ν(CO). Attempts to crystallize compound **5** under an atmosphere of CO were unsuccessful and resulted only in the isolation of **6**.

[Ir(C_8H_{13}){κ^3-*NNB*-B(azaindolyl)$_3$}(CO)] (6)

A sample of [Ir(**Tai**)(COD)] (100 mg, 0.15 mmol) was placed in a Schlenk tube and dissolved in toluene (approx 12 mL) at RT by vigorous stirring to give a bright yellow solution. The flask was then equipped with a septum and CO was bubbled through by means of a balloon while a concurrent small flow of N_2 was maintained. Upon saturation of the reaction mixture with CO, the color changed to an almost colorless solution. The CO was bubbled through the solution for a further 15 min. The CO

atmosphere was removed by purging the flask with N_2. The mixture was filtered through a glass-microfiber filter, the volatiles were then removed under reduced pressure until the volume had reduced to *ca* less than 1 mL. n-Pentane (10 mL) was subsequently added to give a pale precipitate, which was isolated by filtration and dried in vacuum to yield **6**. Yield: 75 mg (72%). Pale yellow crystals of compound **6** were obtained by slow diffusion of n-pentane into a toluene solution of **6**. NMR, δ($C_5D_5CD_3$): ^{1}H (300 MHz), 8.15 (1H, dd, $^4J_{HH}$ = 1.8 Hz, $^3J_{HH}$ = 4.8 Hz, aza), 7.72 (1H, dd, , $^4J_{HH}$ = 1.4 Hz, $^3J_{HH}$ = 3.7 Hz, aza), 7.70 (1H, m, aza), 7.66 (1H, d, $^3J_{HH}$ = 3.7 Hz, aza), 7.55 (1H, dd, $^4J_{HH}$ = 1.1 Hz, $^3J_{HH}$ = 5.5 Hz, aza), 7.32 (1H, d, $^3J_{HH}$ = 3.3 Hz, aza), 7.25 (1H, d, $^3J_{HH}$ = 3.3 Hz, aza), 7.22 (1H, dd, $^4J_{HH}$ = 1.3 Hz, $^3J_{HH}$ = 7.9 Hz, aza), 7.14 (1H, dd, $^4J_{HH}$ = 1.3 Hz, $^3J_{HH}$ = 7.7 Hz, aza), 6.82 (1H, dd, $^3J_{HH}$ = 7.7 Hz, $^3J_{HH}$ = 4.7 Hz, aza), 6.66 (1H, d, $^3J_{HH}$ = 3.7 Hz, aza), 6.40 (1H, dd, $^4J_{HH}$ = 0.7 Hz, $^3J_{HH}$ = 7.7 Hz, aza), 6.39 (1H, dd, $^4J_{HH}$ = 1.3 Hz, $^3J_{HH}$ = 7.9 Hz, aza), 6.29 (1H, d, $^3J_{HH}$ = 3.3 Hz, aza), 6.12 (1H, d, $^3J_{HH}$ = 3.3 Hz, aza), 5.61 (1H, ddd, $^3J_{HH}$ =10.3 Hz, $^3J_{HH}$ = 12.5 Hz, $^3J_{HH}$ = 10.3 Hz, C*H*=CH), 5.45 (1H, ddd, $^3J_{HH}$ = 6.4 Hz, $^3J_{HH}$ = 10.3 Hz, $^3J_{HH}$ = 10.3 Hz, CH=C*H*), 2.11 (1H, m, C_8H_{13}), 1.90 (2H, m, C_8H_{13}), 1.74 (1H, m C_8H_{13}), 1.6 (2H, m, C_8H_{13}), 1.46 (1H. broad m, C_8H_{13}), 1.20 (3H, m, C_8H_{13} including Ir-C*H*), 0.85 (1H, broad m, β-hydrogen, IrC_8H_{13}). ^{13}C{^{1}H} (125 MHz), 173.1 (*C*O), 155.1, 153.1, 152.7, 142.8, 141.6, 138.2, 132.5, 131.6, 130.9, 129.4, 129.3, 128.2, 123.9, 122.4, 121.7, 115.9, 115.5, 114.8, 103.4, 103.2, 102.9 (azaindole, the two CH=CH of the cyclooctenyl moiety are obscured from the solvent signals), 41.6, 29.7, 29.3 27.9, 24.8 (*C*H_2s of cyclooctenyl), 22.7 (Ir-*C*H). ^{11}B{^{1}H}, –9.26 (s, $\Delta\nu_{1/2}$ = 27.9 Hz); ^{11}B, –9.26 (s); IR (neat): 1984 cm^{-1} ν(CO); IR (toluene): 2008 cm^{-1} ν(CO); IR (THF): 2012 cm^{-1} ν(CO); MS (ESI$^+$): 585.1 [M-C_8H_{13}]$^+$, 693.2 [M+H]$^+$, 715.2 [M+Na]$^+$; Elem. Anal.: Found: C 53.89, H 4.20 N 11.30; Calc. for $C_{30}H_{28}BIrN_6O$.1/3 toluene: C 53.76, H 4.28, N 11.63.

[Ir(C_8H_{13}){κ^3-*NNB*-B(azaindolyl)$_3$}(CO)(CNC_8H_9)] (11)

A mixture of **6** (30 mg, 0.043 mmol), 2,6-dimethyl-phenylisocyanide (5.7 mg, 0.043 mmol) and d^8-toluene (ca. 0.6 mL) was prepared in a glovebox. The mixture was transferred to a NMR tube and spectra recorded that showed complete conversion to **11** within a few minutes. The contents of the NMR tube were transferred in a Schlenk tube and volatiles removed under reduced pressure to give a yellow solid that was washed with pentane (5 mL) and dried in vacuum to give **11** as a pale yellow to off-white

solid. Yield: 29 mg (81%). Colorless crystals of **11** were obtained by slow diffusion of n-pentane into a toluene solution of **11**. NMR δ($C_5D_5CD_3$); ^{1}H (300 MHz), 8.26 (1H, dd, $^4J_{HH}$ = 2.2 Hz, $^3J_{HH}$ = 5.1 Hz, aza), 8.25 (1H, dd, $^4J_{HH}$ = 1.5 Hz, $^3J_{HH}$ = 7.7 Hz, aza), 8.20 (1H, d, $^3J_{HH}$ = 4.4 Hz, aza), 7.91 (1H, d, $^3J_{HH}$ = 3.7 Hz, aza), 7.84 (1H, dd, $^4J_{HH}$ = 1.5 Hz, $^3J_{HH}$ = 7.7 Hz, aza), 7.65 (1H, d, $^3J_{HH}$ = 2.9 Hz, aza), 7.32 (3H, m, aza and Ar-NC), 6.85 (2H, m, aza and Ar-NC), 6.71 (1H, d, 3.7 Hz, aza), 6.65 (2H, broad d, aza), 6.47 (2H, two overlapping d, $^3J_{HH}$ = 3.7 Hz, $^3J_{HH}$ = 2.9 Hz, aza), 6.43 (1H, m, aza), 6.37 (1H, m, aza), 5.65 (1H, m, C*H*=CH), 5.46 (1H, m, CH=C*H*), 2.4 (1H, broad, C_8H_{13}), 2.25 (6H, s, CH_3), 2.18 (1H, m, C_8H_{13}), 1.9 (5H, m, C_8H_{13}), 1.53 (1H, broad, C_8H_{13}), 1.35 (1H, m, C_8H_{13}), 1.21 (1H, m, Ir-C*H*), 0.10 (1H, broad, β-hydrogen, IrC_8H_{13}); ^{13}C{^{1}H}(125 MHz), 172.5 (*C*O), 157.5, 157.2, 153.7, 152.7, 142.0, 141.8, 141.7, 135.3, 132.8, 131.3, 131.2, 129.7, 129.3, 129.2, 128.5, 128.4, 127.1, 125.6 123.4, 121.7, 121.4, 115.1, 114.8, 114.7, 103.6, 103.0, 100.5 (azaindole, aromatics of isocyanide and *C*H=*C*H), 45.7, 45.0, 31.7, 29.0 (*C*H_2s, cyclooctenyl), 25.9 (*C*H_2 α to Ir-CH), 18.9 (2,6-(*C*H_3)$_2$-PhNC), 13.6 (Ir-*C*H). The isonitrile Ar-N*C* could not be located; ^{11}B{^{1}H}, 4.34 (s, $\Delta\nu_{1/2}$ = 119.4 Hz); ^{11}B, 4.34 (s); IR (neat): 2275 cm^{-1}, 2131 cm^{-1} ν(NC), 1987 cm^{-1} ν(CO); MS (ESI$^+$): 583.1 [M-ArNC-C_8H_{13}]$^+$, 693.2 [M-ArNC+H]$^+$, 824.0 [M+H]$^+$; Elem. Anal.: Found: C 60.27, H 5.26 N 11.07; Calc. for $C_{39}H_{37}BIrN_7O$.toluene: C 60.39, H 4.96, N 10.72.

[Ir(C_8H_{13}){κ^3-*NNB*-B(azaindolyl)$_3$}(CO)(CNC_4H_9)] (12)

A sample of complex **6** (24.4 mg, 0.035 mmol) was placed in the glove-box in a Young's NMR tube and was dissolved in approximately 0.6 mL of d^8-tol. (solvation can be aided by gentle heating). The solution was removed from the glove-box and of ^{t}BuNC (4.0 μL, d = 0.735 mg/μL; equal to 2.9 mg, 1 mol eq.) was added *via* a microsyringe at RT and the NMR spectra recorded that showed complete conversion to **12**. The contents of the NMR tube were transferred to a Schlenk and volatiles were removed under reduced pressure. The residue was washed with n-pentane (5 mL) and filtered, to give an off-white residue that was dried under reduced pressure. The volume of the filtrate was reduced to *ca.* half and then placed at –30 C to give a second crop of the product. Combined Yield: 22 mg (81 %). ^{1}H-NMR δ($C_6D_5CD_3$): 8.23 (1H, dd, $^4J_{HH}$ = 1.5 Hz, $^3J_{HH}$ = 4.4 Hz, azaindole), 8.16 (2H, br. d, $^3J_{HH}$ = 4.4 Hz, azaindole), 7.89 (1H, d, $^3J_{HH}$ = 3.7 Hz, azaindole), 7.83 (1H, dd, $^4J_{HH}$ = 1.5 Hz, $^3J_{HH}$ = 8.1 Hz,

azaindole), 7.65 (1H, br. s, azaindole), 7.36 (1H, d, $^3J_{HH}$ = 3.7 Hz, azaindole), 7.32 (2H, d, $^3J_{HH}$ = 7.3 Hz), 6.84 (1H, m, azaindole), 6.71 (1H, $^3J_{HH}$ = 3.7 Hz, azaindole), 6.49-6.41 (4H, m, azaindole), 5.64 (1H, m, CH=C*H*), 5.50 (1H, m, C*H*=CH); 2.35 (1H, br. s, cyclooctenyl), 2.02 (1H, br. s, cyclooctenyl), 1.85 (3H, br. s, cyclooctenyl), 1.71 (1H, br. s, cyclooctenyl), 1.25 (3H, br. s, cyclooctenyl + Ir-C*H*), 1.02 (9H, s, (C*H*$_3$)$_3$CNC), 0.15 (1H, br. s, β-hydrogen, IrC$_8$H$_{13}$); ^{13}C{^{1}H}-NMR δ(C$_6$D$_5$CD$_3$): 172.3 (*C*O), 157.5, 157.3, 152.8, 141.9, 141.4, 141.1, 132.8, 131.9, 131.5, 131.2, 129.6, 129.3, 128.4, 127.1, 123.4, 121.6, 121.4, 115.0, 114.7, 114.6, 103.5, 102.9, 100.4 (azaindole and *C*H=*C*H), 57.1 ((CH$_3$)$_3$*C*NC), 45.1, 44.3, 31.6 (*C*H$_2$s cyclooctenyl), 29.8 ((*C*H$_3$)$_3$C-NC), 29.1, 25.8 (*C*H$_2$s cyclooctenyl), 12.5 (Ir-*C*H) the ^{t}BuN*C* signal could not be located; ^{11}B{^{1}H}-NMR δ(C$_6$D$_5$CD$_3$): 3.73 (s, $\Delta\nu_{1/2}$ = 120.7 Hz); ^{11}B-NMR δ(C$_6$D$_5$CD$_3$): 3.73 (s, $\Delta\nu_{1/2}$ = 120.7 Hz); IR (neat): 2148.1 cm^{-1} ν(^{t}BuNC), 1993.7 ν(CO). MS (ESI)$^+$: 583.1 [M – ^{t}BuNC –cyloooctenyl]$^+$, 693.2 [M + H – ^{t}BuNC]$^+$, 776.3 [M + H]$^+$, 858.3 [M + H + 2MeCN]$^+$; Elem Anal. Found: C 55.85; H 5.40; N 11.38. Calc for C$_{35}$H$_{37}$BIrN$_7$O.½ pentane: C 55.55; H 5.35; N 12.09.

[Ir(C$_8$H$_{13}$){κ^3-*NNB*-B(azaindolyl)$_3$}(CO){P(OCH$_2$)$_3$CEt}] (13)

A sample of **6** (45 mg, 0.058 mmol) was placed in an NMR tube and dissolved in d^8-toluene (ca. 0.4 mL). To this was added a solution of P(OCH$_2$)$_3$CEt (9.6 mg, 0.059 mmol) in d^8-toluene (ca. 0.2 mL). This resulted in an immediate color change from yellow to colorless and after a few moments a white precipitate had formed. A ^{11}B-NMR spectrum confirmed the complete conversion to a new product. The contents of the tube were transferred to a small Schlenk tube and n-pentane (3 mL) was added. The resulting suspension was left to stir for 10 min after which time it was filtered and a white solid isolated. Some solid remained in the NMR tube. This was dissolved in DCM (2 mL) and transferred to a second Schlenk and the solvent removed. The white residue was washed with n-pentane (5 mL) and filtered. The NMR spectra of the two crops are identical. Combined yield: 41 mg (83%). Colourless crystals were obtained by either letting a toluene solution of **13** standing for two days at room temperature or by layering a DCM solution of **13** with n-pentane. NMR δ(CD$_2$Cl$_2$); ^{1}H, 8.55 (1H, d, $^3J_{HH}$ = 5.4 Hz, aza), 8.47 (1H, d, $^3J_{HH}$ = 5.1 Hz, aza), 7.94 (1H, d, $^4J_{HH}$ = 3.1 Hz, aza), 7.85 Hz (4H, 2 d AB pattern, $^3J_{HH}$ = 7.0 Hz, $^3J_{HH}$ = 8.4 Hz, aza), 7.63 (2H, dd, $^4J_{HH}$ = 3.1 Hz, $^3J_{HH}$ = 8.4 Hz, aza), 7.25 (1H, $^4J_{HH}$ = 2.7 Hz,

aza), 6.91 (1H, $^{4}J_{HH}$ = 3.1 Hz, $^{3}J_{HH}$ = 7.7 Hz, aza), 6.84 (1H, d, $^{3}J_{HH}$ = 5.7 Hz, aza), 6.81 (1H, d, $^{3}J_{HH}$ = 5.7 Hz, aza), 6.66 (1H, d, $^{4}J_{HH}$ = 2.8 Hz, aza), 6.56 (1H, d, $^{4}J_{HH}$ = 2.8 Hz, aza), 6.51 (1H, d, $^{4}J_{HH}$ = 3.1 Hz, aza), 5.35 (2H, m, C*H*=C*H*), 4.40 (6H, d, $^{3}J_{PH}$ = 3.4 Hz, [P(P(OC*H*$_2$)$_3$CEt]), 2.05-1.45 (5H, m, C_8H_{13}), 1.3 (2H, C_8H_{13} + 2H, [P(OCH$_2$)$_3$CC*H*$_2$CH$_3$], q, $^{3}J_{HH}$ = 7.7 Hz), 0.9 (2H, C_8H_{13} + 3H, P(OCH$_2$)$_3$CCH$_2$C*H*$_3$, t, $^{3}J_{HH}$ = 7.7 Hz), 0.7 (1H, m, C_8H_{13}), -0.6 (1H, br. s., β-hydrogen, IrC_8H_{13}); ^{13}C{^{1}H} (75 Hz): 172.3 (*C*O), 157.9, 157.3, 152.2, 144.9, 144.4, 141.5, 133.9, 131.1, 131, 130.5, 130.4, 129.7, 129.3, 127.2, 123.4, 121.1, 120.9, 115.7, 115.3, 114.9, 103.8, 102.8, 100.1 (azaindole and *C*H=*C*H), 74.1 (d, $^{2}J_{PC}$ = 5.8 Hz, [P(O*C*H$_2$)$_3$CCH$_2$CH$_3$]), 43.8, 43.5 (*C*H$_2$ cyclooctenyl), 37.1 (d, $^{3}J_{PC}$ = 28.5 Hz, [P(OCH$_2$)$_3$*C*CH$_2$CH$_3$]), 31.5, 28.5 (*C*H$_2$ cyclooctenyl), 24.4 (P(OCH$_2$)$_3$C*C*H$_2$CH$_3$), 13.1 and 7.5 (P(OCH$_2$)$_3$CCH$_2$*C*H$_3$ and Ir-*C*H); ^{11}B{^{1}H}, 4.2 (d, $^{2}J_{PB}$ = 127 Hz); ^{11}B, 4.2 (d, $^{2}J_{PB}$ = 127 Hz); ^{31}P{^{1}H}, 97.8 (s, br $\Delta\nu_{1/2}$ = 429 Hz); IR (neat): 2013 cm^{-1} ν(CO); ES^{+}: 583.1 [M-C_8H_{13}-phosphite]$^{+}$, 693.2 [M+H-phosphite]$^{+}$, 855.3 [M+H]$^{+}$, 881.2 [M+2H+OMe]$^{+}$, 885.3 [M+H+MeOH]$^{+}$; Elem. Anal. Found: C 54.23; H 5.23; N 9.34. Calc for $C_{36}H_{39}N_6BIrPO_4$.toluene: C 54.60; H 5.01; N 8.88.

Reaction mixture involving [Ir(C_8H_{12}){κ^3-*NNH*-(Ph)HB(azaindolyl)$_2$}] (15) and CO

A sample of [Ir(**^{Ph}Bai**)(COD)] (24 mg, 0.038 mmol) was placed in a Young's NMR tube and dissolved ca. 0.6 mL of C_6D_6. The tube was connected to a vacuum line and the inert atmosphere removed by two freeze-thaw cycles. The solution was allowed to equilibrate at RT and the NMR tube was connected to a CO cylinder and pressurized to ca. 1.5 bar. This mixture was vigorously shaken under the dynamic positive pressure. After a few minutes the color of the solution changed to almost colorless and the NMR tube was removed from the CO supply.

Complexes **16**, **17** and **18** were observed spectroscopically in an approximate ratio of 55%, 25% and 20% as determined by integration.[50] Although, three signals should be expected in the boron NMR spectra of this mixture, only two could be distinguished. The most intense signal was located at 6.0 ppm (^{11}B{^{1}H}-NMR δ($C_5D_5CD_3$)) in the spectrum and corresponds to complex **16** (see below). The second signal was found at 2.4 ppm. It is likely, given its intensity that the third signal is underneath the signal at 6.0 ppm. It is currently unclear whether the signal at 2.4 ppm corresponds to **17** or **18**. IR spectrum of the mixture (toluene): 2078 cm^{-1} , 2061 cm^{-1}, 2010 cm^{-1}, 1989 cm^{-1} ν(CO). Selected data for: Ir(η^1-

C_8H_{13})$(CO)_2${κ^3-*NNB*-(Ph)B(azaindolyl)$_2$) (**16**), ^{1}H-NMR (500 MHz) δ(C_6D_6): 5.65 (1H, m, C*H*=C*H*), 5.52 (1H, m, C*H*=C*H*), 2.13-1.09 (a series of multiplet signals overlapping with signals for **18**, 10H, cyclooctenyl), –0.21 (1H, broad s, β-hydrogen, IrC_8H_{13}); ^{13}C{^{1}H}-NMR (125 MHz) δ(C_6D_6): 46.2, 44.8, 32.2, 29.8, 27.0 (*C*H_2s of cyclooctenyl), 18.5 (Ir-*C*H); ^{11}B{^{1}H}-NMR δ($C_5D_5CD_3$): 6.0 (s, $\Delta\nu_{1/2}$ = 190 Hz); ^{11}B-NMR δ($C_5D_5CD_3$): 6.0 (s, , $\Delta\nu_{1/2}$ = 190 Hz); Ir(H)$(CO)_2${κ^3-*NNB*-(Ph)B(azaindolyl)$_2$) (**17**), ^{1}H-NMR (500 MHz) δ(C_6D_6): –14.5 (1H, s, Ir–H); Ir(σ^1,η^2-C_8H_{13})(CO){κ^3-*NNB*-(Ph)B(azaindolyl)$_2$) (**18**): ^{1}H-NMR (500 MHz) δ(C_6D_6): 3.89 (1H, m, C*H*=CH), 3.28 (1H, m, CH=CH), 2.72 (1H, m, β-hydrogen, IrC_8H_{13}), 2.42 (1H, m, CH_2), 2.13-1.09 (a series of mutiplet signals overlapping with signals for **16**, 9H, cyclooctenyl); ^{13}C{^{1}H}-NMR (125 MHz) δ(C_6D_6): 59.7 (CH=CH), 49.8 (CH_2), 46.1 (CH=CH), 36.3, 29.8, 27.3, 27.0 (*C*H_2s of cyclooctenyl), 15.7 (Ir-*C*H).

Attempts to isolate pure samples from this mixture proved challenging and only small quantities of complexes **19** and **20** were obtained. Complex **19** was isolated as follows: All volatiles were removed from the mixture and the residue extracted with pentane. A yellow solid precipitated from the solution after a period of 2 h at –80 °C. Complex **20** was isolated as follows: After removing all volatiles the residue was washed with pentane. The resulting solid was re-dissolved in toluene, filtered again and the volume reduced to approx 2 mL. Slow diffusion of pentane into this solution gave a small amount of crystalline material suitable for X-ray analysis.

Data obtained for [Ir(η^1-C_8H_{13}){κ^3-*NNB*-(Ph)B(azaindolyl)$_2$}(CO)] (**19**): ^{1}H-NMR (300 MHz) δ($C_5D_5CD_3$): 7.86 (2H, dd, $^3J_{HH}$ = 8.1 Hz, $^4J_{HH}$ = unresolved, azaindole), 7.72 (1H, d, $^3J_{HH}$ = 5.1 Hz, azaindole), 7.56 (H, d, $^3J_{HH}$ = 5.1 Hz, azaindole), 7.36 (4H, m, *o*/*m*-phenyl), 7.26 (2H, two overlapping signals, azaindole and *p*-phenyl), 7.20 (1H, d, $^3J_{HH}$ = 8.8 Hz, azaindole), 6.42 (2H, m, azaindole), 6.31 (1H, d, $^3J_{HH}$ = 2.9 Hz, azaindole), 6.14 (1H, d, $^3J_{HH}$ = 2.9 Hz, azaindole), 5.70 (1H, m, C*H*=CH), 5.46 (1H, m, CH=C*H*), 2.16 (1H, m, cyclooctenyl), 1.89 (2H, m, cyclooctenyl), 1.70 (1H, m cyclooctenyl), 1.57 (2H, m, cyclooctenyl), 1.46 (1H. br. m, cyclooctenyl), 1.28 (3H, m, cyclooctenyl and Ir-C*H*), 1.02 (1H, br. m, β-hydrogen, IrC_8H_{13}); ^{11}B{^{1}H}-NMR δ($C_5D_5CD_3$): –5.2 (s, hhw. = 190 Hz); ^{11}B-NMR: –5.2 (s, hww. = 200 Hz). Data obtained for [Ir(H){κ^3-*NNB*-(Ph)B(azaindolyl)$_2$}(CO)] (**20**): ^{11}B{^{1}H}-NMR δ($C_5D_5CD_3$): –2.6 (br, s, hhw. = 310 Hz).

Supporting Information i) Additional experimental details including the synthesis of the deuterium labeled ligand salts and complexes; ii) full details concerning the computation investigations including further information and iii) full details concerning the crystallographic studies together with additional selected bond distances and angles. This material is available free of charge via the Internet at http://pubs.acs.org.

Acknowledgements G.R.O. gratefully acknowledges the award of a Royal Society Dorothy Hodgkin Research Fellowship from the Royal Society. The authors would like to thank the Leverhulme Trust (N. T.) and EPSRC (A. H.) for funding, Johnson Matthey for the loan of the iridium salts and Dr. C. P. Butts for his help with the NMR studies.

References

1 Hill, A. F.; Owen, G. R.; White, A. J. P.; Williams, D. J. *Angew. Chem., Int. Ed*., **1999**, *38*, 2759.

2 Garner, M.; Reglinski, J.; Cassidy, I.; Spicer, M. D.; Kennedy, A. R. *Chem. Commun.,* **1996**, 1975.

3 a) King, R. B. *Adv. Chem. Ser.,* **1967**, *62*, 203. b) Green, M. L. H. *J. Organomet. Chem.,* **1995**, *500*, 127.

4 (a) Owen, G. R. *Chem. Soc. Rev.* **2012**, *41*, 3535. (b) Braunschweig, H.; Dewhurst, R. D., *Dalton Trans*. **2011**, *40*, 549. (c) Amgoune, A.; Bourissou, D., *Chem. Commun*. **2011**, *47*, 859. (d) Bouhadir, G.; Amgoune, A.; Bourissou, D. *Adv. Organomet. Chem*. **2010**, *58*, 1. (e) Owen, G. R., *Transition Met. Chem.* **2010**, *35*, 221. (f) van der Vulgt, J. I. *Angew. Chem. Int. Ed.* **2010**, *49*, 252. (g) Braunschweig, H.; Dewhurst, R. D.; Schneider, A. *Chem. Rev.* **2010**, *110*, 3924. (h) Kuzu, I.; Krummenacher, I.; Meyer, J; Armbruster, F.; Breher, F. *Dalton Trans.,* **2008**, 5836. (i) Fontaine, F.-G.; Boudreau, J.; Thibault, M.-H. *Eur. J. Inorg. Chem.,* **2008**, 5439.

5 a) Hill, A. F. *Organometallics* **2006**, *25*, 4741; b) Parkin, G. *Organometallics* **2006**, *25*, 4744.

6 Although some examples were previously reported, they were later disproved see: a) Shriver, D. F. *J. Am. Chem. Soc.* **1963**, *85*, 3509; b) Parshall, G. W. *J. Am. Chem., Soc.* **1964**, *86*, 361; c) Johnson, M. P.; Shriver, D. F. *J. Am. Chem. Soc.* **1966**, *88*, 301; d) Braunschweig, H.; Wagner, T.; *Chem. Ber.* **1994**, *127*, 1613; e) Braunschweig, H.; Wagner, T. *Z. Naturforsch. B.* **1996**, *51*, 1618; f) Braunschweig, H.; Kollann, C. *Z. Naturforsch. B.* **1999**, *54*, 839; f) Burlitch, J. M.; Leonowicz, M. E.; Peterson, R. B.; Hughes, R. E. *Inorg. Chem.* **1979**, *18*, 1097; g) Cook, K. S.; Piers, W. E.; McDonald, R. *Organometallics* **1999**, *18*, 1575; h) Cook, K. S.; Piers, W. E.; McDonald, R. *Organometallics* **2001**, *20*, 3927; i) Cook, K. S.; Piers, W. E.; McDonald, R. *J. Am. Chem. Soc.* **2002**, *124*, 5411.

7 The only examples of a pure κ^2*LB* coordination mode, i.e. those which do not feature additional metal–ligand interactions, have been reported by Bourissou; see: (a) Bontemps, S.; Bouhadir, G.; Miqueu, K.; Bourissou, D. *J. Am. Chem. Soc.* **2006**, *128*, 12056. For examples further supported by arene coordination see: (b) Sircoglou, M.; Bontemps, S.; Mercy, M.; Miqueu, K.; Ladeira, S.; Saffon, N.; Maron, L.; Bouhadir, G.; Bourissou, D. *Inorg. Chem.* **2010**, *49*, 3983.

8 Selected recent examples: (a) Zech, A.; Haddow, M. F.; Othman, H.; Owen, G. R. *Organometallics,* **2012**, *31*, 6753. (b) Crossley, I. R.; Hayes, J. *J. Organomet. Chem.* **2012**, *716*, 285. (c) Dyson, G; Zech, A.; Rawe, B. W.; Haddow, M. F.; Hamilton, A.; Owen, G. R. *Organometallics,* **2011**, *30*, 5844. (d) López-Gómez, M. J.; Connelly, N. G.; Haddow, M. F.; Hamilton, A.; Lusi, M.; Baisch, U.; Orpen, A. G. *Dalton Trans.* **2011**, *40*, 4647. (e) Nuss, G.; Saischek, G.; Harum, B. N.; Volpe, M.; Belaj, F.; Moesch-Zanetti, N. C. *Inorg. Chem.* **2011**, *50*, 12632. (f) Nuss, G.; Saischek, G.; Harum, B. N.; Volpe, M.; Gatterer, K.; Belaj, F.; Moesch-Zanetti, N. C. *Inorg. Chem.* **2011**, *50*, 1991. (g) Owen, G. R.; Gould, P. H.; Hamilton, A.; Tsoureas, N. *Dalton Trans.* **2010**, *39*, 49. (h) López-Gómez, M. J.; Connelly, N. G.; Haddow, M. F.; Hamilton, A.; Orpen, A. G. *Dalton Trans.* **2010**, *39*, 5221. (i) Crossley, I. R.; Hill, A. F.; Willis, A. C. *Organometallics,* **2010**, *29*, 326. (j) Owen, G. R.; Gould, P. H.; Charmant, J. P. H.; Hamilton, A.; Saithong, S. *Dalton Trans.* **2010**, *39*, 392.

9 Selected recent examples: (a) Kameo, H.; Hashimoto, Y.; Nakazawa, H. *Organometallics* **2012**, *31*, 4251. (b) Kameo, H.; Hashimoto, Y.; Nakazawa, H. *Organometallics* **2012**, *31*, 3155. (c) Suess, D. L. M.; Tsay, C.; Peters, J. C. *J. Am. Chem. Soc.* **2012**, *134*, 14158. (d) Harman, W. H.; Peters, J. C. *J. Am. Chem. Soc*. **2012**, *134*, 5080. (e) Moret, M.-E.; Peters, J. C. *J. Am. Chem. Soc.* **2011**, *133*, 18118. (f) Moret, M.-E.; Peters, J. C. *Angew. Chem. Int. Ed.* **2011**, *50*, 2063. (g) Conifer, C. M.; Law, D. J.; Sunley, G. J.; White, A. J. P.; Britovsek, G. J. P. *Organometallics* **2011**, *30*, 4060. (h) Kameo, H.; Nakazawa, H. *Organometallics,* **2012**, *31*, 7476. (i) Anderson, J. S. Moret, M.-E. Peters, J. C. *J. Am. Chem. Soc.* **2013**, *135*, 534.

10 (a) Tsoureas, N.; Kuo, Y.-Y.; Haddow, M. F.; Owen, G. R. *Chem. Commun*. **2011**, *47*, 484. (b) Tsoureas, N.; Haddow, M. F.; Hamilton, A.; Owen, G. R. *Chem. Commun.* **2009**, 2538. (c) Tsoureas, N.; Bevis, T.; Butts, C. P.; Hamilton, A.; Owen, G. R. *Organometallics,* **2009**, *28*, 5222

11 For a review on boron coordination supported by π-ligand interactions see: Emslie, D. J. H.; Cowie, B. E.; Kolpin, K. B. *Dalton Trans.* **2012**, *41*, 1101.

12 (a) Bauer, J.; Braunschweig, H.; Dewhurst, R. D. *Chem*. *Rev*. **2012**, *112*, 4329. (b) Bauer, J.; Bertermann, R.; Braunschweig, H.; Gruss, K.; Hupp, F.; Kramer, T. *Inorg*. *Chem*. **2012**, *51*, 5617. (c) Tschersich, C.; Limberg, C.; Roggan, S.; Herwig, C.; Ernsting, N.; Kovalenko, S.; Mebs, S. *Angew. Chem. Int. Ed.* **2012**, *51*, 4989. (d) Lin, T.-P.; Ke, I.-S.; Gabbai, F. P. *Angew. Chem. Int. Ed.* **2012**, *51*, 4985. (e) Bauer, J. Braunschweig, H.; Damme, A.; Gruss, K.; Radacki, K. *Chem*. *Commun*. **2011**, *47*, 12783. (f) Rudd, P. A.; Liu, S.; Gagliardi, L.; Young, V. G.; Lu, C. C. *J. Am. Chem. Soc.* **2011**, *133*, 20724. (g) Martincova, J.; Dostal, L.; Herres-Pawlis, S.; Ruzicka, A.; Jambor, R. *Chem*.- *Eur. J.* **2011**, *17*, 7423. (h) Wade, C. R.; Gabbai, F. P. *Angew. Chem. Int. Ed.* **2011**, *50*, 7369. (i) Brendler, E.; Waechtler, E.; Heine, T.; Zhechkov, L.; Langer, T.; Poettgen, R.; Hill, A. F.; Wagler, J. *Angew. Chem. Int. Ed.* **2011**, *50*, 4696. (j) Wade, C. R.; Lin, T.-P.; Nelson, R. C.; Mader, E. A.; Miller, J. T.; Gabbai, F. P. *J. Am. Chem. Soc.* **2011**, *133*, 8948. (k) Derrah, E. J.; Sircoglou, M.; Mercy, M.; Ladeira, S.; Bouhadir, G.; Miqueu, K.; Maron, L.; Bourissou, D. *Organometallics* **2011**, *30*, 657. (l) Bauer, J.; Braunschweig, H.; Brenner, P.; Kraft, K.; Radacki, K.; Schwab, K. *Chem.-Eur. J.* **2010**, *16*, 11985. (m)

Wagler, J.; Heine, T.; Hill, A. F. *Organometallics* **2010**, *29*, 5607. (n) Gualco, P.; Mercy, M.; Ladeira, S.; Coppel, Y.; Maron, L.; Amgoune, A.; Bourissou, D. *Chem.- Eur. J.* **2010**, *16*, 10808. (o) Lin, T.-P.; Wade, C. R.; Perez, L. M.; Gabbai, F. P. *Angew. Chem. Int. Ed.* **2010**, *49*, 6357. (p) Gualco, P.; L., T.-P.; Sircoglou, M.; Mercy, M.; Ladeira, S.; Bouhadir, G.; Perez, L. M.; Amgoune, A.; Maron, L.; Gabbai, F. P.; Bourissou, D. *Angew. Chem. Int. Ed.* **2009**, *48*, 9892. (q) Sircoglou, M.; Mercy, M.; Saffon, N.; Coppel, Y.; Bouhadir, G.; Maron, L.; Bourissou, D. *Angew. Chem. Int. Ed.* **2009**, *48*, 3454.

13 Rudolf, G. C.; Hamilton, A.; Orpen, A. G.; Owen, G. R. *Chem. Commun.*, **2009**, 553.

14 (a) Song, D.; Jia, W. L.; Wu, G.; Wang, S. *Dalton Trans.,* **2005**, 433. (b) Saito, T.; Kuwata, S.; Ikariya, T. *Chem. Lett.,* **2006**, *35*, 1224. (c) Owen, G. R.; Tsoureas, N.; Hamilton, A.; Orpen, A. G. *Dalton Trans.,* **2008**, 6039.

15 Pettinari, C.; in *Scorpionates II:* Chelating Borate Ligands, Imperial College Press, London, 2008.

16 Peters later reported a system where a nickel–borane complex was similarly '*recharged*' with hydrogen providing a second example and further confirmation that this methodology could be utilized to provide active hydrogenation catalysts. See reference 9d. See also: Zeng, G.; Sakaki, S. *Inorg. Chem.* **2013**, *52*, 2844.

17 (a) Owen, G. R.; Tsoureas, N.; Hope, R. F.; Kuo, Y.-Y.; Haddow, M. F. *Dalton Trans.* **2011**, *40*, 5906. (b) Tsoureas, N.; Nunn, J.; Bevis, T.; Haddow, M. F.; Hamilton, A.; Owen, G. R. *Dalton Trans.* **2011**, *40*, 951. (c) Tsoureas, N.; Hope, R. F.; Haddow, M. F.; Owen, G. R. *Eur. J. Inorg. Chem*, **2011**, 5233.

18 A mono 7-azaindolyl substituted borohydride species which acts as a ligand has also previously been reported: Wagler, J. Hill, A. F. *Organometallics*, **2008**, *27*, 2350.

19 Recent examples (a) Fawcett, J.; Harding, D. A. J.; Hope, E. G.; Singh, K.; Solan, G. A. *Dalton Trans*. **2010**, *39*, 10781. (b) Hallett, A. J.; Adams, C. J.; Anderson, K. M.; Baber, R. A.; Connelly, N.

G.; Prime, C. J. *Dalton Trans*. **2010**, *39*, 5899. (c) Fortman, G. C.; Slawin, A. M. Z.; Nolan, S. P. *Dalton Trans*. **2010**, *39*, 3923. (d) Pawlikowski, A. V.; Gray, T. S.; Schoendorff, G.; Baird, B.; Ellern, A.; Windus, T. L.; Sadow, A. D. *Inorg. Chem. Acta*. **2009**, *362*, 4517. (e) Dabb, S. L.; Ho, J. H. H.; Hodgson, R.; Messerle, B. A.; Wagler, J. *Dalton Trans*. **2009**, 634.

20 The spectrum of **6** revealed 19 sharp signals corresponding to three inequivalent azaindole units and 2 olefinic carbons between 102.9 and 155.1 ppm (two signal corresponding to carbon atoms in the azaindole ring were obscured by the signals of the toluene solvent). In addition, six resonances in the alkyl region between 41.6 and 22.7 ppm (*c.f.* 46.2 and 17.0 ppm for **5**) were observed.

21 There were two independent molecules in the unit cell of the crystals obtained of this compound.

22 In the case of **6-d$_1$,** the signals at 1.48 and 2.00 ppm showed NOE's with azaindole signals at 7.54 and 7.17 ppm, respectively in the ROESY experiments. An inspection of the crystal structure of **6** suggests that these interactions as those resulting from syn addition across the double bond.

23 Crossley, I. R.; Foreman, M. R. St.-J.; Hill, A. F.; Owen, G. R.; White, A. J. P.;Williams, D. J.; Willis, A. C. *Organometallics*, **2008**, *27*, 381.

24 A survey of the literature reveals no examples of strong sigma donor ligands such as hydride and alkyl groups in the coordination site trans to boron. In the same way, there are only a handful of cases where a π-acceptor ligands is located trans to the boron center (see references 8d, 9a,b,f, 23 and 25a). In all of these cases the alternative coordination site, if one is available, is occupied by a hydride ligand or another π-acceptor ligand.

25 (a) Figueroa, J. S.; Melnick, J. G.; Parkin, G. *Inorg. Chem.* **2006**, *45*, 7056. (b) Crossely, I. R.; Hill, A. F.; Willis, A. C. *Organometallics*, **2006**, *25*, 289. (c) Crossely, I. R.; Hill, A. F.; Willis, A. C. *Organometallics*, **2008**, *27*, 312.

26 One possible explanation for such observation is related to the relative stabilization of certain geometries: see reference 4e.

27 Heitsch, C. W.; Verkade, J. G. *Inorg. Chem*. **1962**, *1*, 453.

28 Stahl, L.; Trakarnpruk, W.; Freeman, J. W.; Arif, A. M.; Ernst, R. D. *Inorg. Chem.* **1995**, *34*, 1810.

29 Tolman, C. A. *Chem. Rev*. **1977**, *77*, 313.

30 Jover, J.; Fey, N.; Harvey, J. N.; Lloyd-Jones, G. C.; Orpen, A. G.; Owen-Smith, G. J. J; Murray, P.; Hose, D. R. J.; Osborne, R.; Purdie, M. *Organometallics*, **2010**, *29*, 6245.

31 This is true for periods up to ca. 48 h after which time there were indications of decomposition and crystalline material consisting of $Ir_4(CO)_{12}$ were obtained.

32 The signals in the ^2H NMR spectrum were particularly broad and accordingly the chemical shifts quoted are tentative. Given the unambiguous assignment of complexes **5-d$_1$** and **6-d$_1$**, it is reasonable to assume that the deuterium atoms are located in the β positions in **16-d$_1$** and **18-d$_1$**.

33 Our previous investigations have revealed that the ^{11}B NMR signals of the boron nuclei in compounds containing the **^{Ar}Bai** (Ar = phenyl, mesityl, naphthyl) ligands tend to be significantly broader.

34 In this case the PPh_3 ligand is cis to the boron in $[Rh\{B(mt)_3\}PPh_3]$ and trans to the boron in $[Rh\{B(mt)_3\}PPh_3(CO)]$ and the chemical shift will also be effected by the change in the position of the phosphorus ligand. The ^{11}B NMR chemicals shifts for the two complexes are –0.19 ppm and 7.45 ppm respectively.

35 Aubke, K.; Wang, C. *Coord. Chem. Rev.,* **1994**, *137*, 483.

36 (a) Elliott, P. I. P.; Haslam, C. E.; Spey, S. E.; Haynes, A. *Inorg. Chem.* **2006**, *45*, 6269. (b) Tanke, R. S.; Crabtree, R. H. *Inorg. Chem*. **1989**, *28*, 3444.

37 (a) Sattler, W.; Parkin, G. *Chem. Commun.* **2009**, 7566. (b) Werner, H. *Angew. Chem. Int. Ed.*. **1990**, *29*, 1077. (c) Treichel, P. M. *Adv. Organomet. Chem*. **1983**, *11*, 21. (d) Singleton, E.; Oosthuizen, H. E. *Adv. Organomet. Chem.* **1983**, *22*, 209.

38 For a recent examples of the cyclooctenyl ligand coordinating to an iridium center with 1-σ,4,5-η^2-C_8H_{13} coordination mode see: Nguyen, D. H.; Pérez-Torrente, J. J.; Lomba, L.; Jiménez, M. V.; Lahoz, F. J.; Oro, L. A. *Dalton Trans.* **2011**, *40*, 8429.

39 Martín, M.; Sola, E.; Torres, O.; Plou, P.; Oro, L. A. *Organometallics,* **2003**, *22*, 5406.

40 A search was performed with ConQuest.1.14 on the Cambridge Structural Database (5.33), with updates up until August 2012.

41 Cordero, B.; Gómez, V.; Platero-Prats, A. E.; Revés, M.; Echeverría, J.; Cremades, E.; Barragán, F.; Alvarez, S. *Dalton Trans.* **2008,** 2832.

42 Yih, K. -H.; Hamdemir, I. K.; Mondloch, J. E.; Bayram, E.; Özkar, S.; Vasić, R.; Frenkel, A. I.; Anderson, O. P.; Finke, R. G. *Inorg. Chem.* **2012**, *51*, 3186.

43 (a) Seino, H.; Saito, A.; Kajitani, H.; Mizobe, Y. *Organometallics*, **2008**, *27*, 1275. (b) Wang, H. H.; Casalnuovo, A. L.; Johnson, B. J.; Mueting, A. M.; Pignolet, L. H. *Inorg. Chem.* **1988**, *27*, 325. (c) Casalnuovo, A. L.; Pignolet, L. H.; Van der Velden, J. W. A.; Bour, J. J.; Steggerda, J. J. *J. Am. Chem. Soc.* **1983**, *105*, 5957. (d) Wang, H. H.; Pignolet, L. H. *Inorg. Chem.* **1980**, *19*, 1470.

44 A search on the Cambridge Structural Database was carried out - see reference 40. Of the 101 complexes featuring the "Ir–C≡N" fragment, there were two examples containing longer Ir–C distances than in **11**. See: (a) Lacey, P.; Sykes, A. G. *J. Coord. Chem.* **2003**, *56*, 141. (b) Mague, J. T. **1992**, *11*, 677.

45 A search on the Cambridge Structural Database was carried out - see reference 40. Of the 50 complexes featuring the "Ir–P$(OC)_3$" fragment, there was one complex containing a longer Ir–P distance than in **13**. See: Kanematsu, N.; Ebihara, M.; Kawamura, T. *Inorg. Chim. Acta.* **2001**, *323*, 96.

46 When calculations were performed focusing on the corresponding associative mechanism, involving the corresponding octahedral intermediate, the structure optimized directly to **4i$_{calc}$**.

47 (a) Crossley, I. R.; Hill, A. F.; Willis, A. C. *Organometallics* **2005**, *24*, 1062. (b) Landry, V. K.; Melnick, J. G.; Bucella, D.; Pang, K.; Ulichny, J. C.; Parkin, G. *Inorg. Chem.* **2006**, *45*, 2588.

48 Crossley, I. R.; Hill, A. F.; Willis, A. C. *Dalton Trans.* **2008**, 201.

49 The Ru•••B distance in **3** (2.12 Å) was significant shorter than the Ir•••B distance in **TS1**. This may be related to a number of factors including the different supporting heterocycles, the additional agostic interaction between the benzyl group and the ruthenium center or the fact that the S–Ru–S angle is 166.13(4)°.

50 The aromatic region of the spectra involving the mixture **16**, **17** and **18** involves 39 chemical environments (45 H in total) and was rather complicated. We were therefore unable to assign these signals with any degree of confidence. For the same reason the proton assignments given for the aliphatic region of the spectra are tentative and based on the analogous compounds containing the **Tai** ligand.

Graphical Abstract

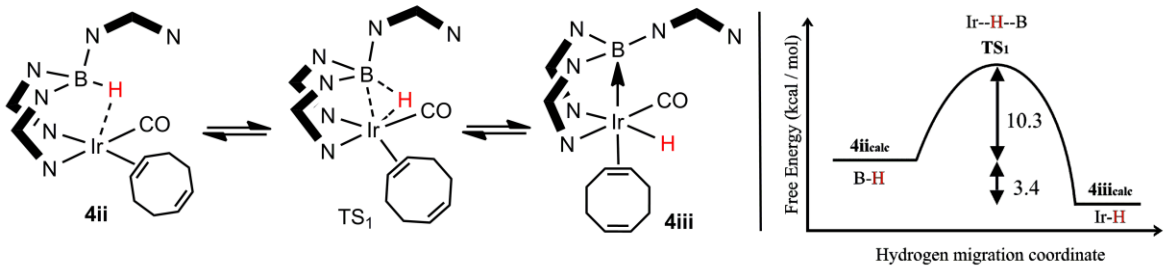

Hydrogen migration (B-H to Ir-H) - *Low energy barrier - Small energy difference*